Nuclear Physics Mid Term Plan in Italy

LNF – Session

Frascati, December 1st - 2nd 2022

Detectors for X radiation

Marco Miliucci

Laboratori Nazionali di Frascati, INFN

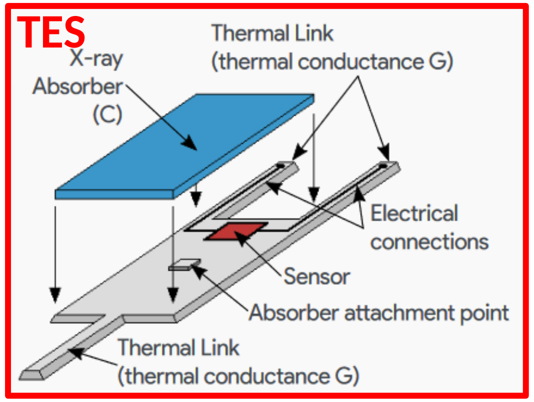

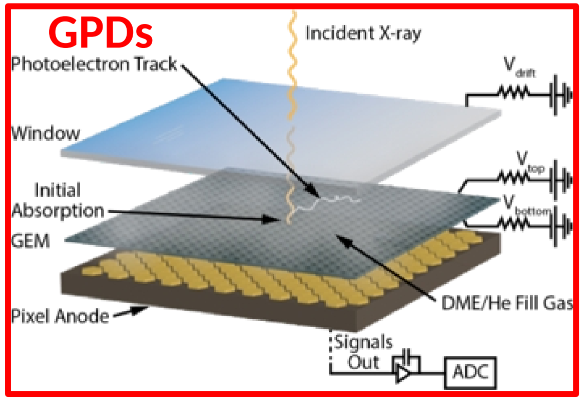

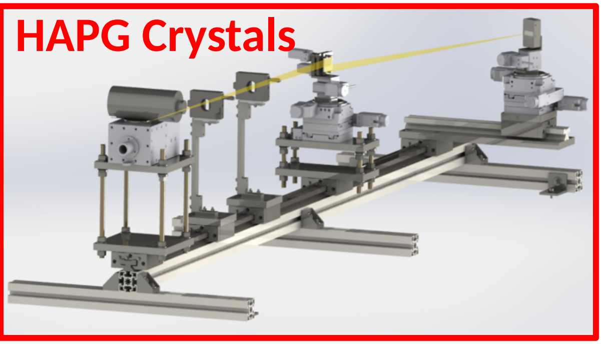

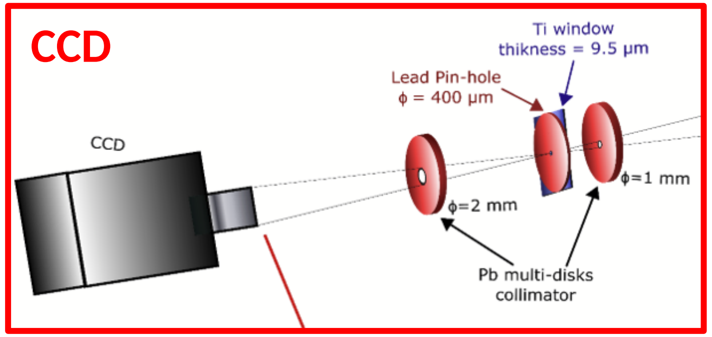

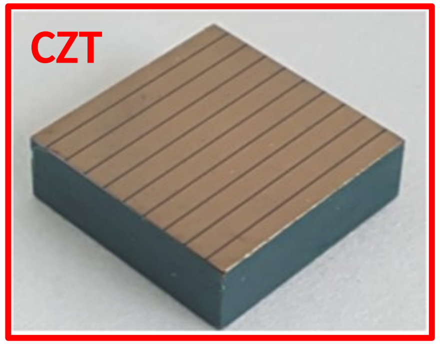

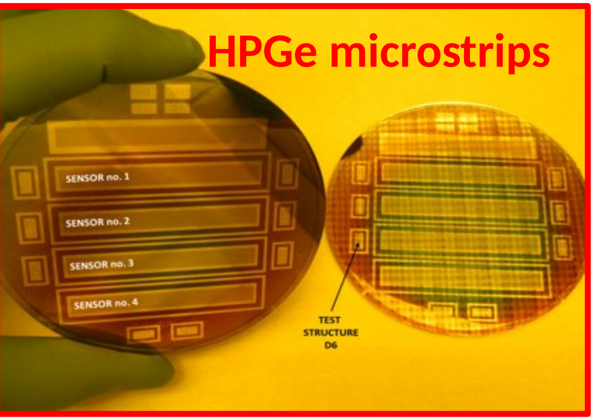

Hybrid Detectors
Microstrips/ pixels

Whole X-ray energy range

+

Different detection methods

+

Excellent features

<u>WIDE CHOICE</u>

<u>FOR</u>

<u>SEVERAL APPLICATIONS</u>

A. Manfreda, Pisa (INFN)

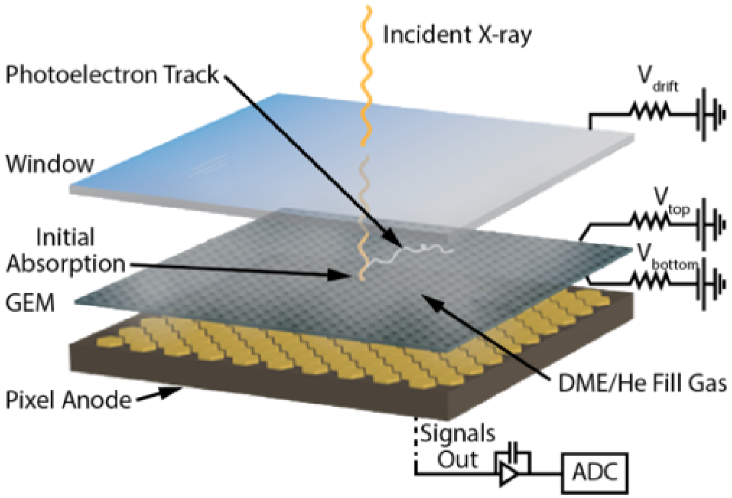

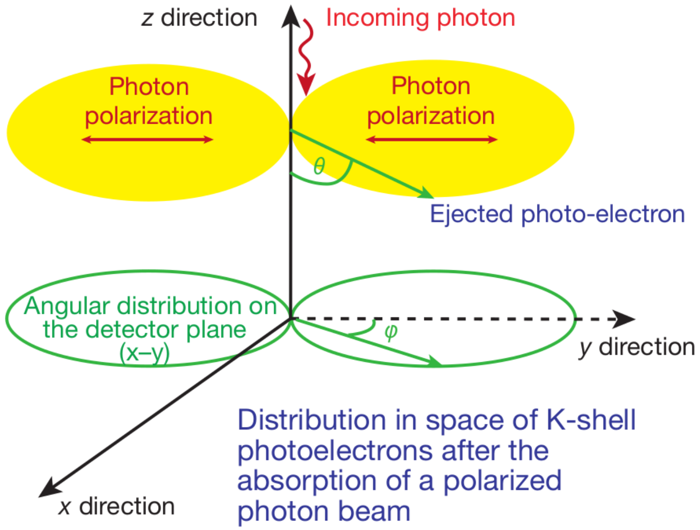

$$\frac{d\sigma_C^K}{d\Omega} \propto Z^5 E^{-\frac{7}{2}} \frac{\sin^2\theta\cos^2\phi}{(1+\beta\cos\theta)^4}$$

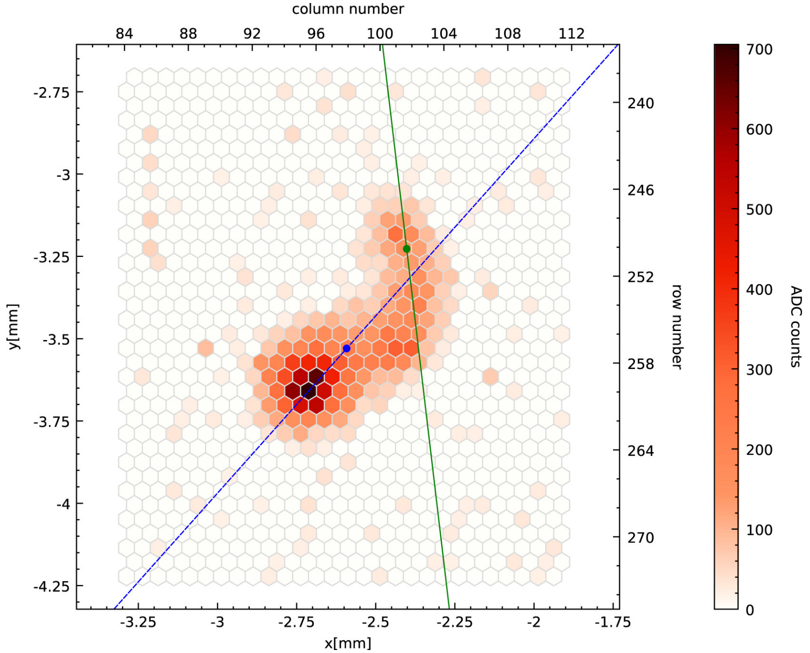

- Image of the photoelectron ionization tracks on a finely segmented anode, in the plane orthogonal to the incoming radiation
  -> source imaging, linear polarization degree and angle
- Overcomes the Bragg diffraction and Scattering based polarimeters (narrow active area, rotation...)
- Custom ASIC: self-triggering, each pixel (50 µm) pitch acts both as anode as well as first stage of the readout chain
- High intrinsic degree of symmetry (hexagonal grid), no detector rotation required
- The charge is measured as the sum of the charge in all the pixels composing the main track

Costa et al., Nature 411 (2001)
Bellazzini et al., Nucl. Instr. Methods A, 566 (2006)

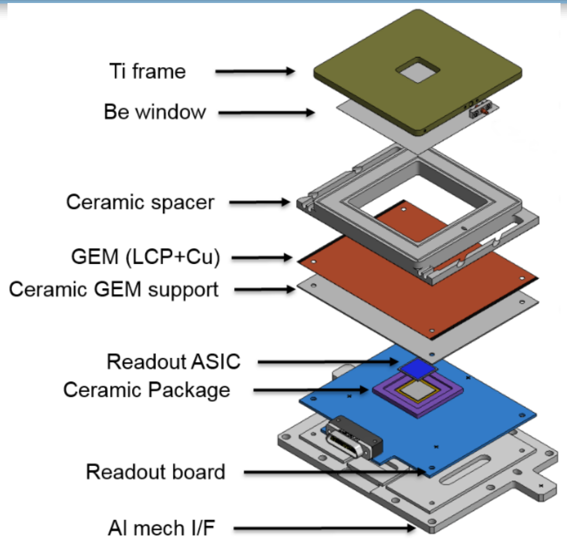

Sealed detector: no gas system required, ideal for long space missions

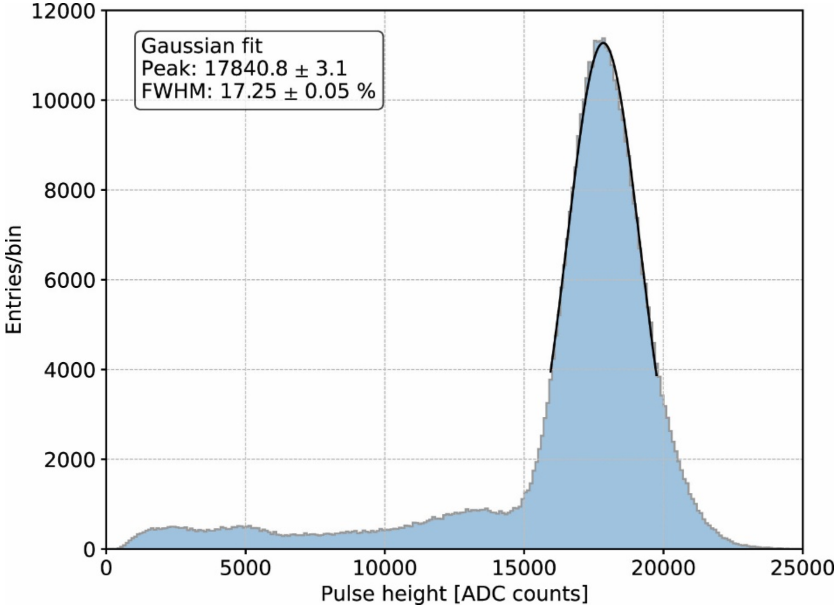

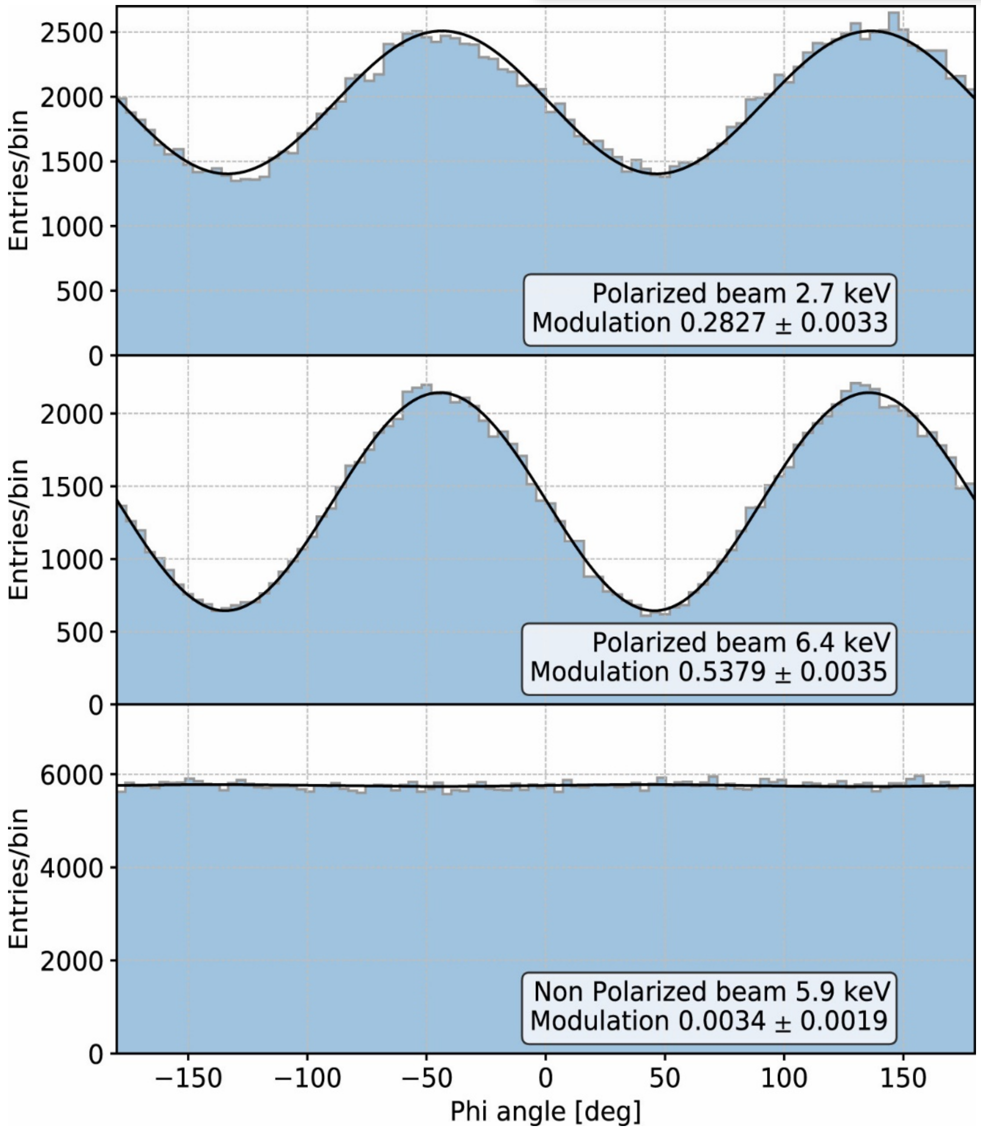

Baldini et al, Astroparticle Physics 133 (2021)

- 17% FWHM @5.9 keV
- μ = 0.54 @6.4 keV
  0.28 @2.7 keV
- ε > 20% @2.0 keV
- ~1 ms dead time

The quality of a polarimeter is measured by the modulation factor μ, which is a number between 0 and 1 that measure how modulated is the instrument response to a 100% polarized beam

A new era for X-ray polarimetry (IXPE)

The capability to perform polarimetry resolved in energy, time/phase and space has proven to be **crucial for discriminating between different astrophysical models**

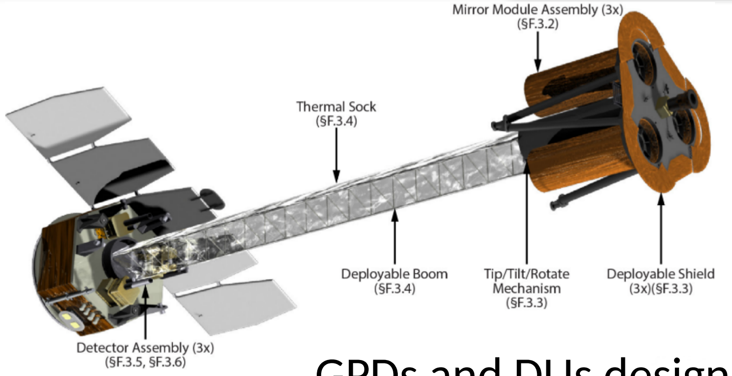

GPDs and DUs designed and assembled by INFN

- **2017: The Imaging X-Ray Polarimetry Explorer (IXPE) mission is selected**
  - Funded by NASA-ASI partnership
  - Completely dedicated to X-ray polarimetry
  - GPDs are the enabler technology
- **2018: PolarLight**
  - First GPD to operate successfully in space on a demonstrator mission (without X-ray optics)
    [Feng, Bellazzini Nature Astronomy, 4 (2020)]
- **2021, December: IXPE launch**
  - First light in January 2022
    [Soffitta et al, AJ 162 (2021)]
  - Almost 1 year of successful space operations

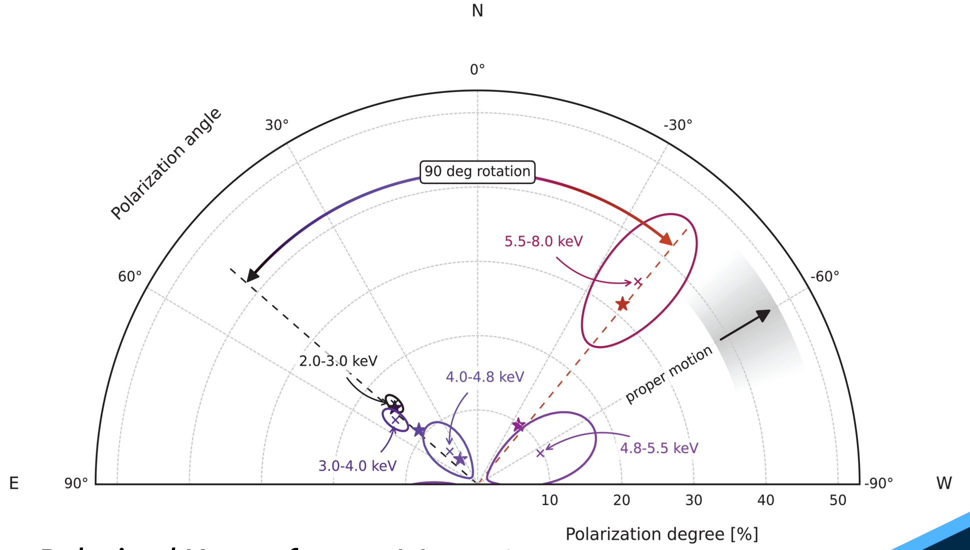

Polarized X-rays from a Magnetar
Taverna et al., Science 378, 6620 (2022)

M. Borri, STFC-Daresbury Laboratory - UKRI

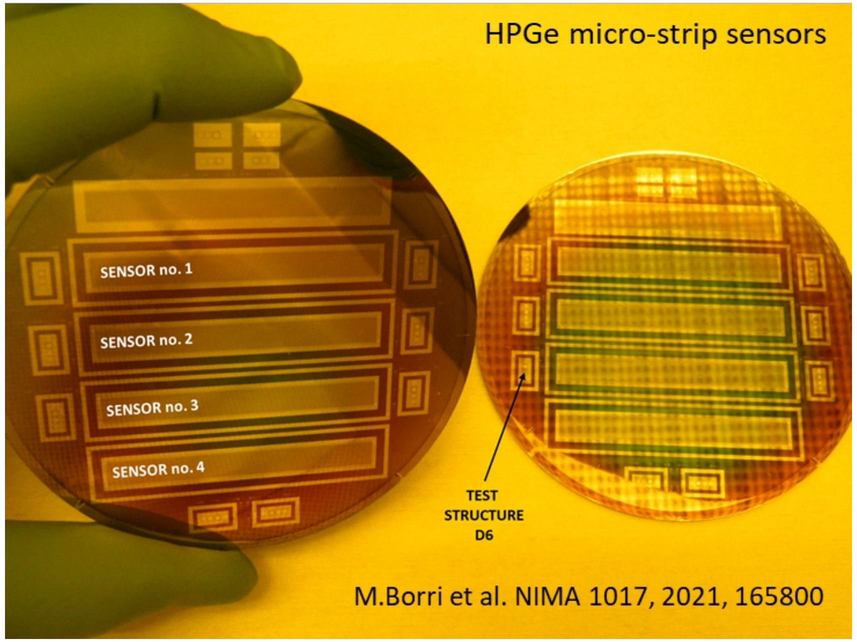

Commercial sensor integration into detector system

The XH detector system

5-40 keV working range
Charge integration concept

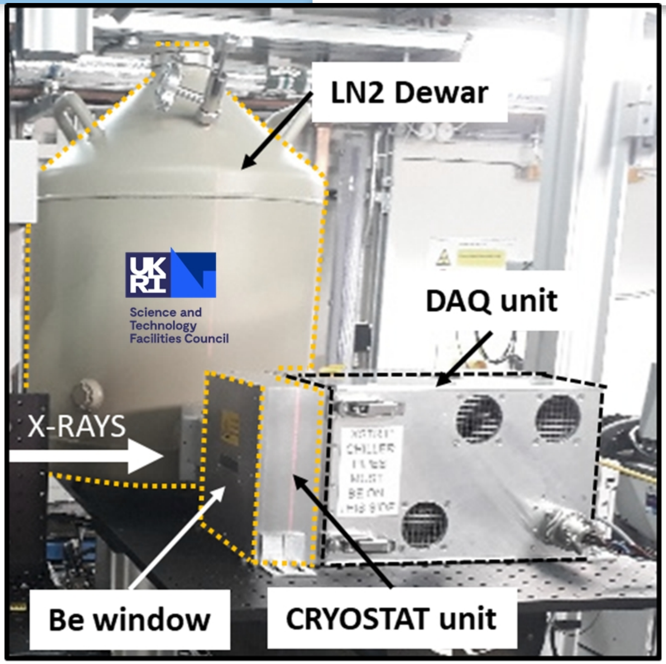

LN_2 Dewar connected to one HPGe sensor (T<-170C)

Custom made front-end electronics (10-14W, T>-40C)

Custom made cryostat (8 ASICS for readout)

Size: 1024 Strips

Strip pitch: 50 µm

Strip Length: 5 mm

Sensor Thickness: 1.5 mm

Two Guard-Rings

Interleaved Wire-Bonding Pads

Back Illuminated

Conceptual sketch of the detector system electronics

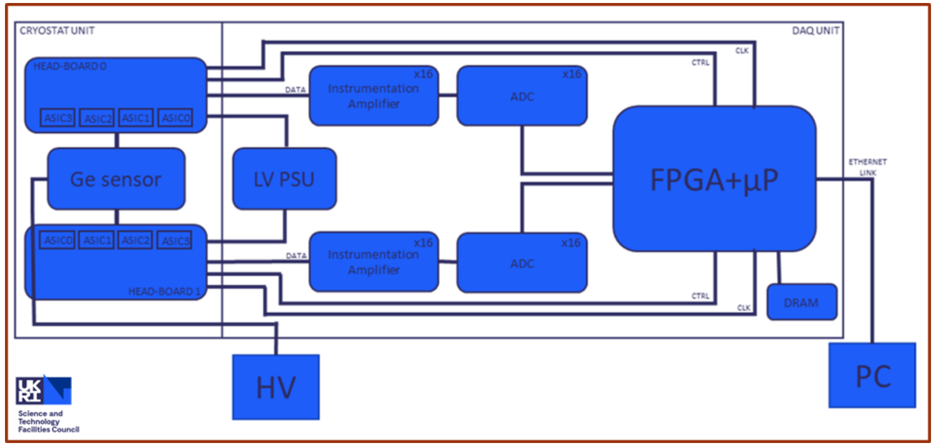

- HPGe crystals provide a unique combination of favourable crystal properties and material purity.

- This translates into a material with high and uniform detection efficiency.

- As well as an excellent energy resolution over a large area (wafer Ø 90mm).

- Selected as a suitable option to detect hard X-rays in **radiation harsh environments.**

- <u>Target instantaneous flux: **~2*10^9 γ/s/mm^2**</u>

Property	Units	Value
Atomic number		32
Cubic structure		face-centered diamond-cubic
Density	g cm^{-3}	5.32
Band gap	eV	0.66 (indirect)
Pair creation energy	eV	2.96
Electron mobility	cm^2 V^{-1} s^{-1}	3900
Hole mobility	cm^2 V^{-1} s^{-1}	1900

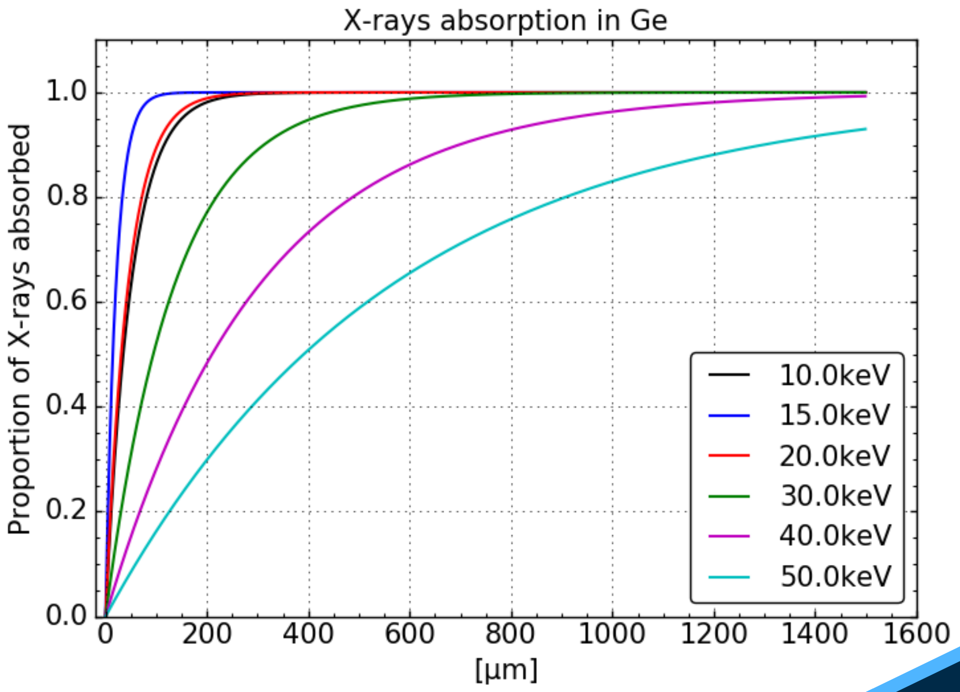

- Energy dispersive absorption spectroscopy.

- An experimental technique to determine the chemical and physical structure of a sample by analysing modulations within its X-ray absorption spectrum.

- **Particularly suitable for experiments using the pump & probe technique.**

- The system (called XH) is currently deployed at the ID24 High Power Laser Facility (HPLF) at the Extremely Brilliant Source ESRF (EBS-ESRF).

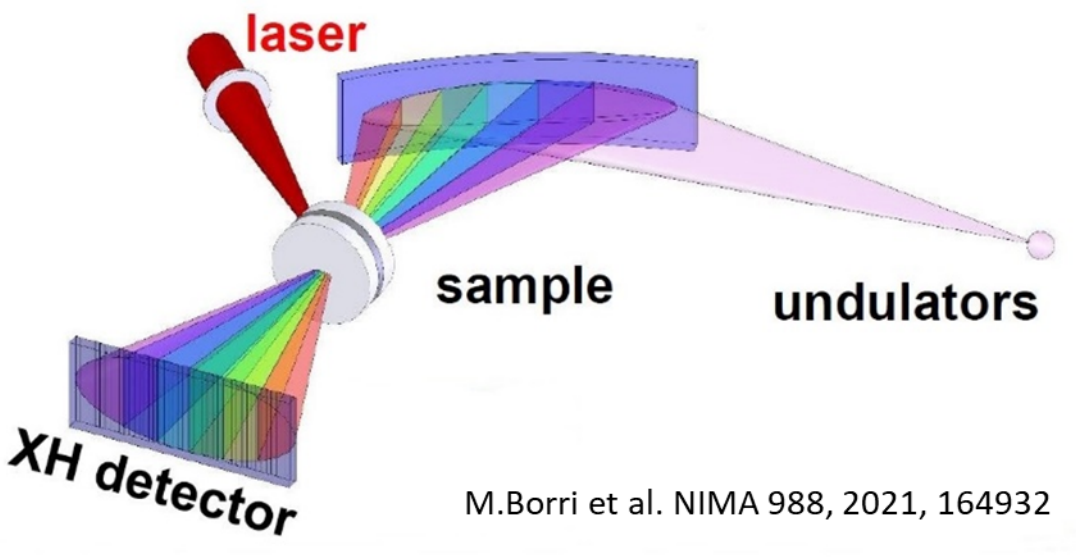

M.Borri et al. NIMA 988, 2021, 164932

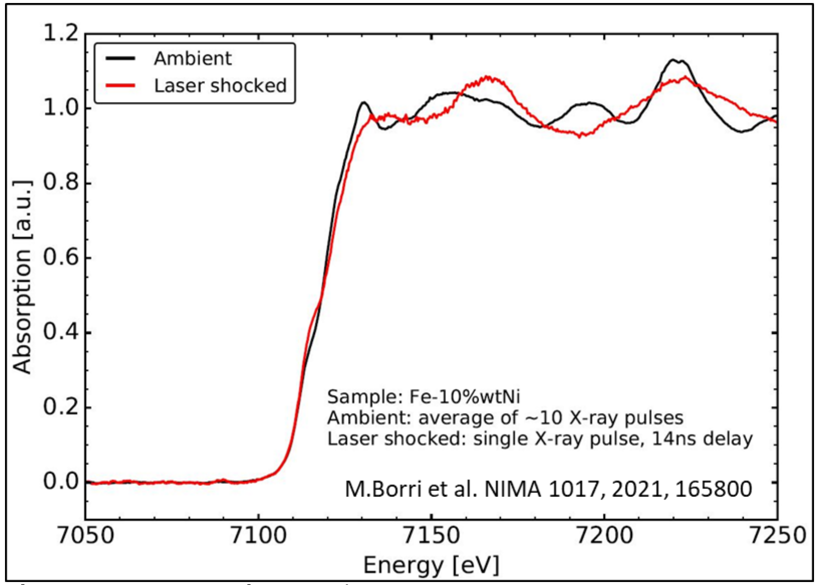

M.Borri et al. NIMA 1017, 2021, 165800

Using the laser probe, samples are driven into an almost “plasma” phase where the lattice structure is destroyed

Torchio, R., Occelli, F., Mathon, O. et al.
Probing local and electronic structure in Warm Dense Matter: single pulse synchrotron x-ray absorption spectroscopy on shocked Fe.
*Sci Rep **6**, 26402 (2016).* https://doi.org/10.1038/srep26402

A. Giachero, Milano - Bicocca

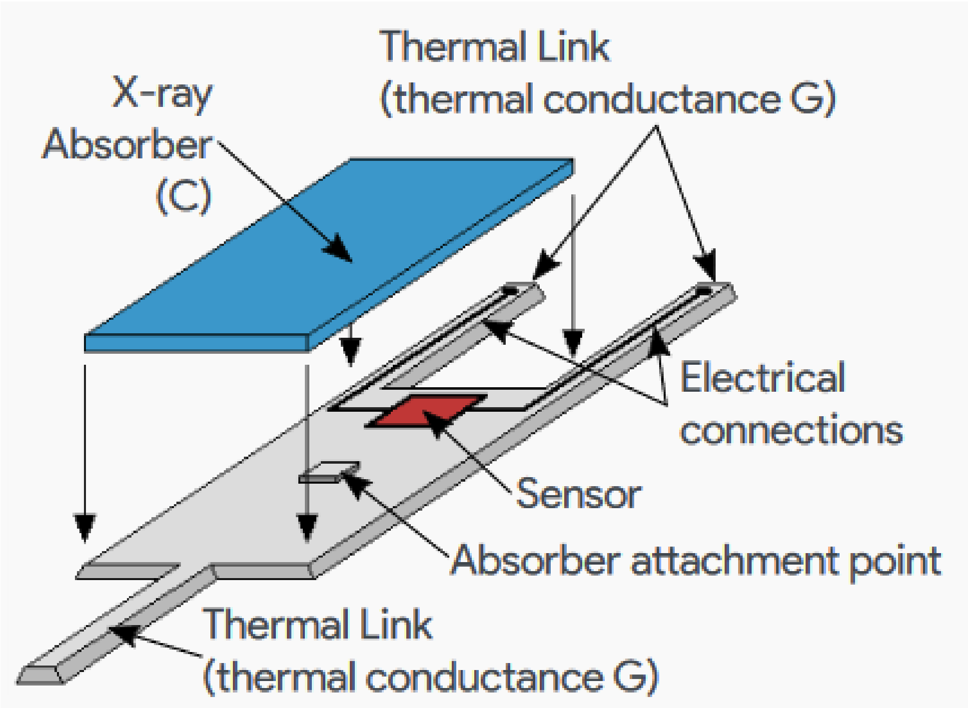

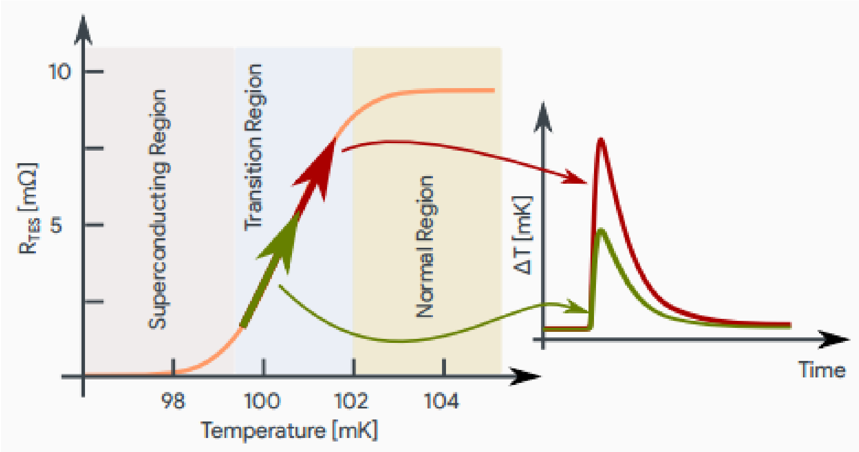

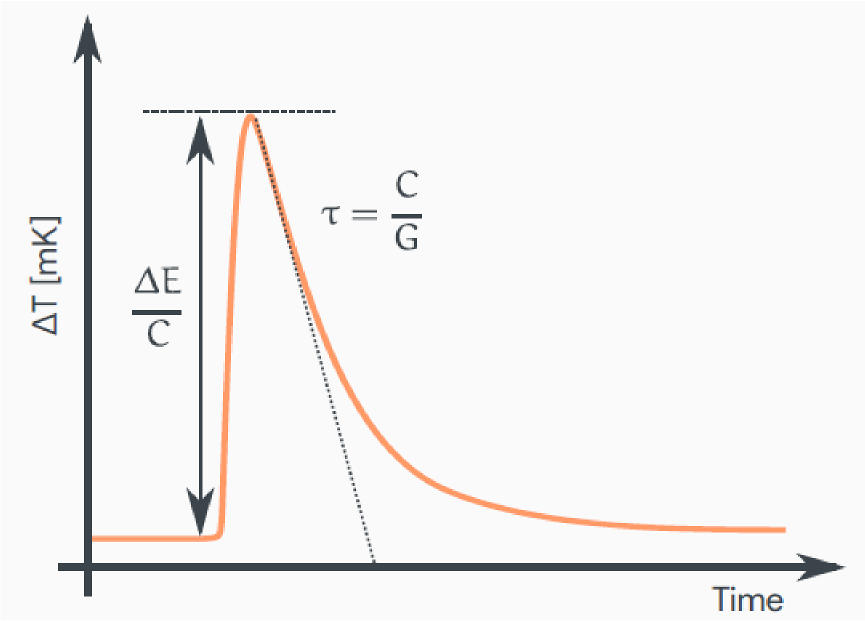

A Low Temperature Calorimeter senses the heat generated by a particle/photon absorbed and thermalized in a very low heat capacity element

Complete energy thermalization:
ionization->excitation->heat->calorimetry;

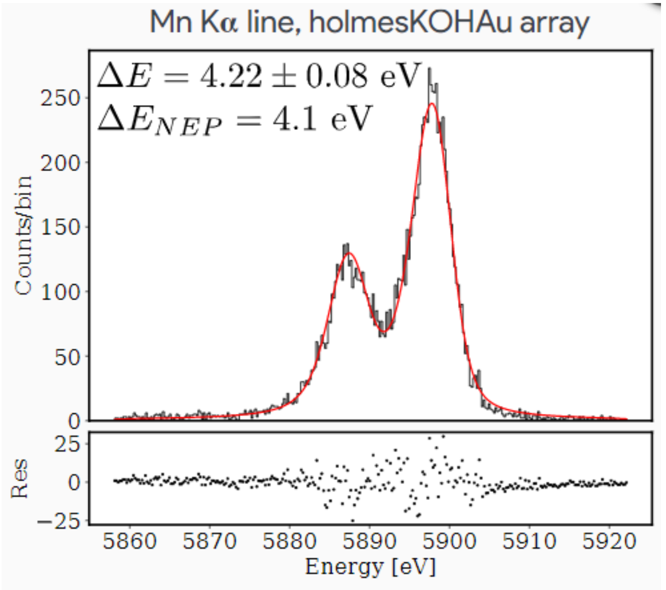

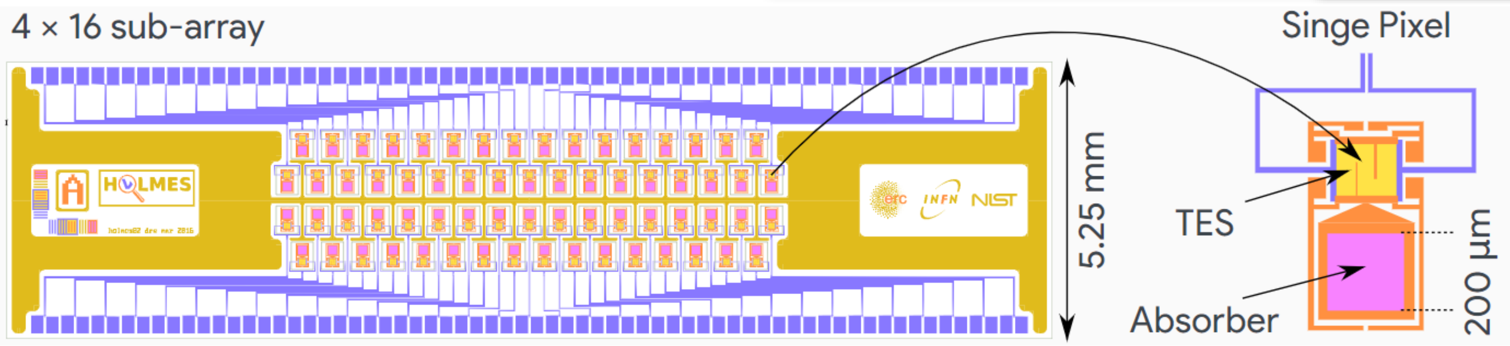

Sensor: TES Mo/Cu bilayers, critical temperature Tc=100 mK;
Absorber: Gold, 2um thick for full e/γ absorption;

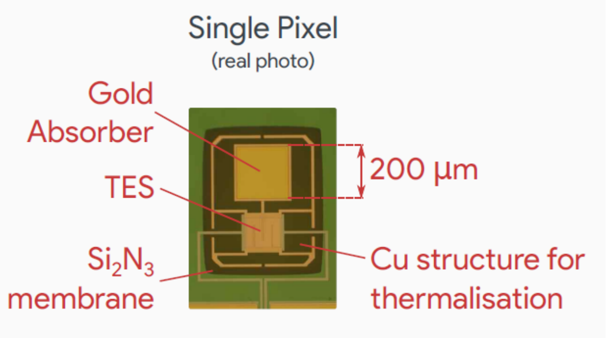

- Pixel activity of AEC ~ 300 Bq/det;
- Energy resolution: eV in the keV range
- Time resolution: µs;

Small size ⇒ low thermal capacity C ⇒ excellent energy resolution:

The energy of single x-ray photon can be measured with resolving powers: $E/\Delta E > 10^3$ ⇒ relative energy resolutions $\Delta E(\%) < ‰$

$$\Delta E_{FWHM} = \begin{cases} 0.75\text{ eV @ }1.25\text{ keV} & \text{IEEE Trans Appl Supercond. 29,5 (2019) 2100605} \\ 0.90\text{ eV @ }1.50\text{ keV} & \text{IEEE Trans Appl Supercond. 23,3 (2013) 2100705} \\ 1.58\text{ eV @ }5.90\text{ keV} & \text{J. Low Temp. Phys. 167 (2012) 168–175} \\ 1.96\text{ eV @ }8.00\text{ keV} & \text{J. Low Temp. Phys. 167 (2012) 168–175} \end{cases}$$

The negative electro-thermal feedback provides a fast time response;

Large array ($>10^3 - 10^5$) in different applications
astrophysical observation, beamline spectroscopy, x-ray tomography, etc;

$$@2.6\text{ keV}: \Delta E_{FWHM} \simeq 3-4\text{ eV}, \; \tau_{rise} \simeq 10\,\mu s, \; \tau_{decay} \simeq 100\,\mu s$$

more details on J. Ullom and D. Bennet
Supercond. Sci. Technol. 28 (2015) 084003
and L. Gottardi * and K. Nagayashi
Appl. Sci. 11 (2021) 3793

Limit to energy resolution ⇒ statistical fluctuation of internal energy ⇒ $\Delta E_{rms} = \sqrt{k_B T^2 C}$;

The HOLMES experiment will perform a direct measurement of the neutrino mass by using TES micro calorimeter with ^{163}Ho-implanted absorber;

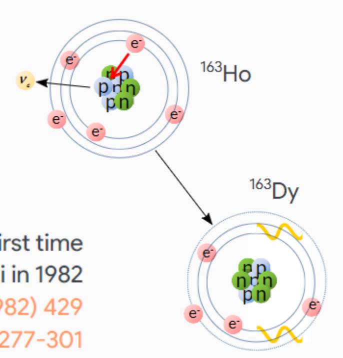

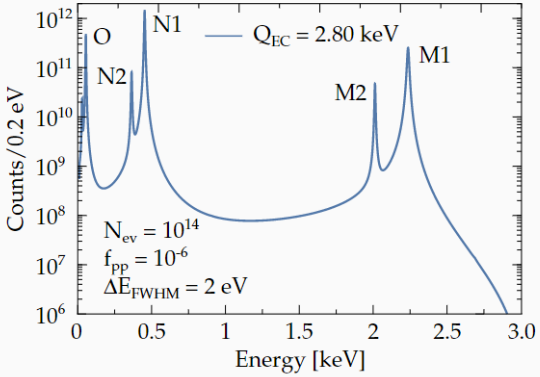

- Electron capture from shell $\geq$ M1 $\Rightarrow$ $^{163}\text{Ho} + e^- \rightarrow {}^{163}\text{Dy}^* + \nu_e(E_c)$;
- End-point shaped by $\sqrt{(Q - E_e)^2 - m_\nu^2}$ (the same of the β-decay);
- Searching for a tiny deformation caused by a non-zero neutrino mass to the spectrum near its end point;
- Calorimetric measurement of Dy atomic de-excitations (mostly non-radiative)

$\Rightarrow$ measurement of the entire energy released except the ν energy;

proposed for the first time by A. De Rujula e M. Lusignoli in 1982
Phys. Lett. 118B (1982) 429
Nucl. Phys. B219 (1983) 277-301

more details on A. Nucciotti
Adv. High En. Phys. 2016 (2016) 9153024
and M. Galeazzi *et al.*
arXiv:1202.4763 [physics.ins-det]

$Q_{EC} = 2.833\,\text{keV}$
$\tau_{1/2} \simeq 4570$ years

J-PARC E62 setup

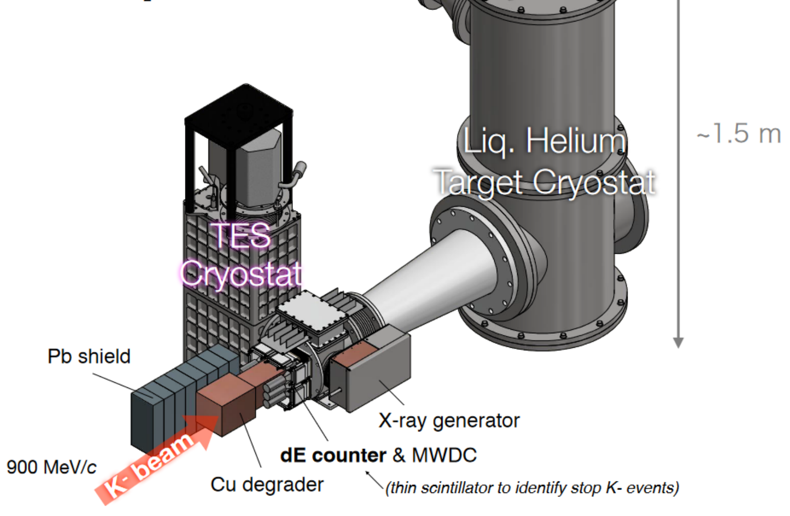

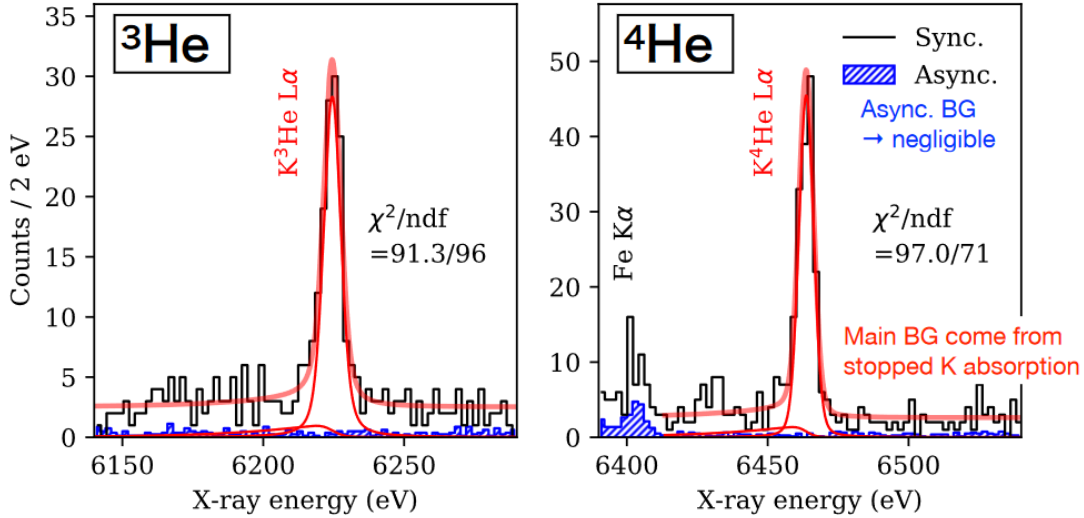

$$E_{3d\to 2p}^{K^{-3}\text{He}} = 6224.5 \pm 0.4(\text{stat}) \pm 0.2(\text{syst})\ \text{eV}$$
$$\Gamma_{2p}^{K^{-3}\text{He}} = 2.5 \pm 1.0(\text{stat}) \pm 0.4(\text{syst})\ \text{eV}$$

$$E_{3d\to 2p}^{K^{-4}\text{He}} = 6463.7 \pm 0.3(\text{stat}) \pm 0.1(\text{syst})\ \text{eV}$$
$$\Gamma_{2p}^{K^{-4}\text{He}} = 1.0 \pm 0.6(\text{stat}) \pm 0.3(\text{syst})\ \text{eV}$$

Groundbreaking high-resolution measurement of K^{3,4}He isotopic shift on 2p level

A. Scordo – LNF

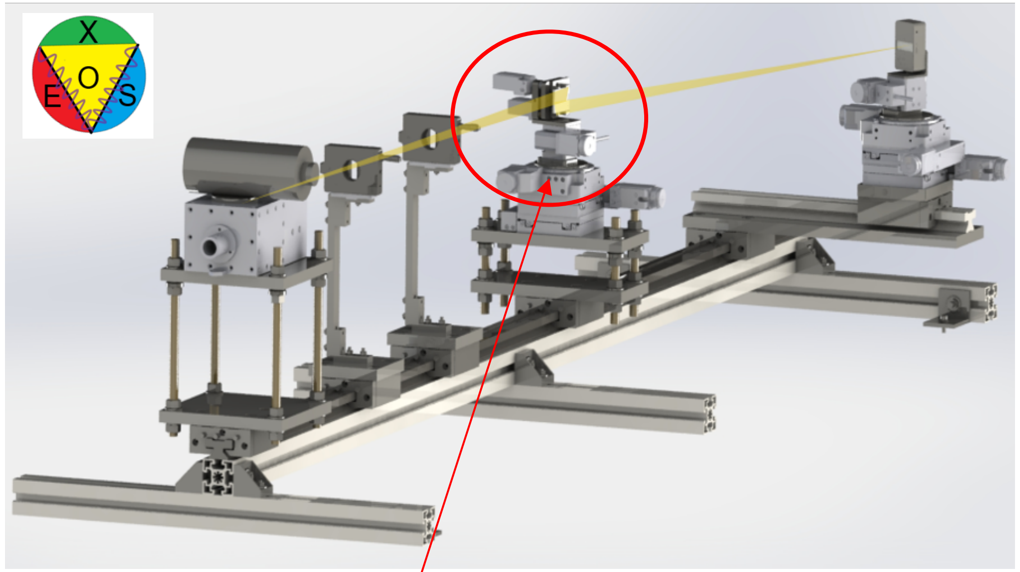

HAPG/HOPG Crystal

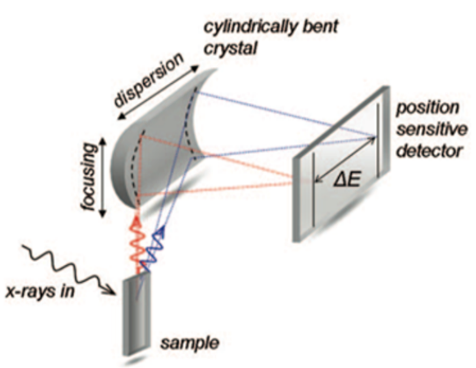

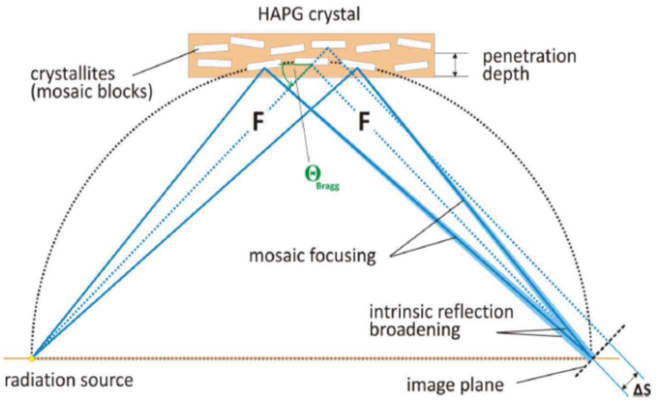

HAPG mosaic crystals in Von Hamos configuration:

- Higher intrinsic reflectivity wrt standard crystals
- VH configuration to exploit sagittal focusing

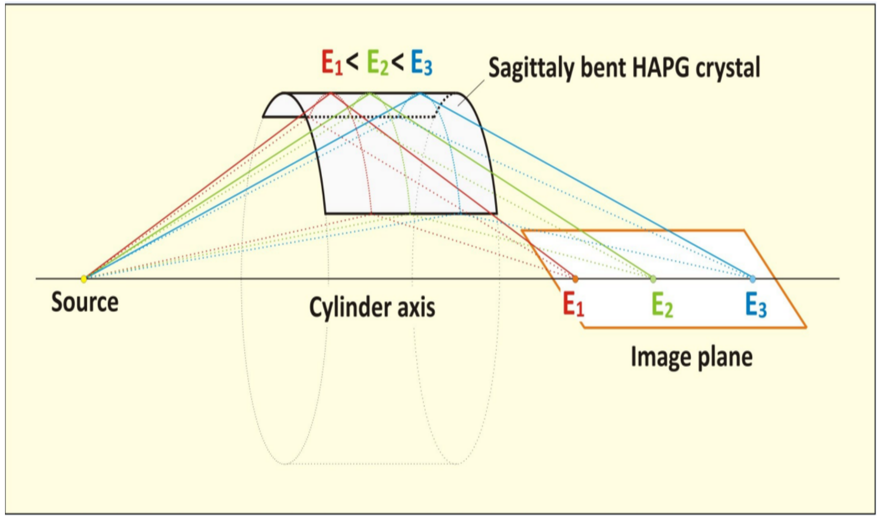

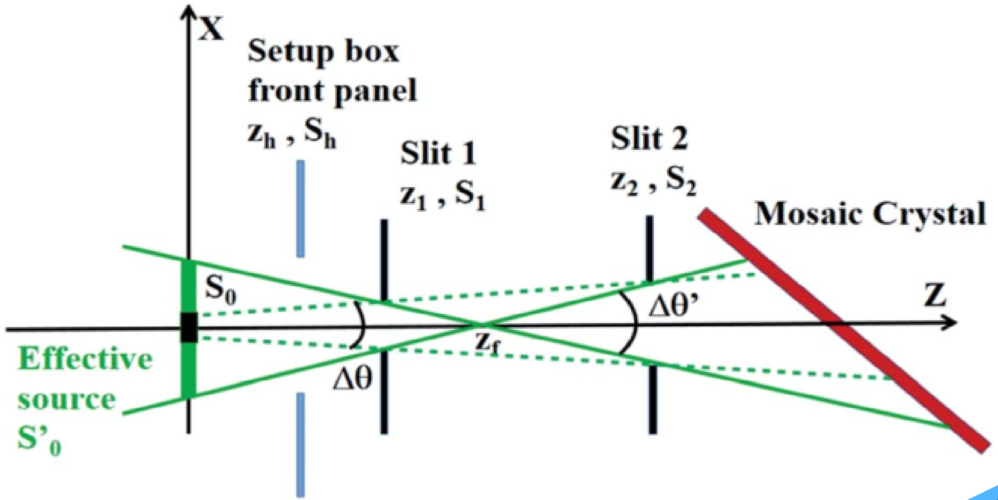

Goal:
FWHM ~ eV
With millimetric sources

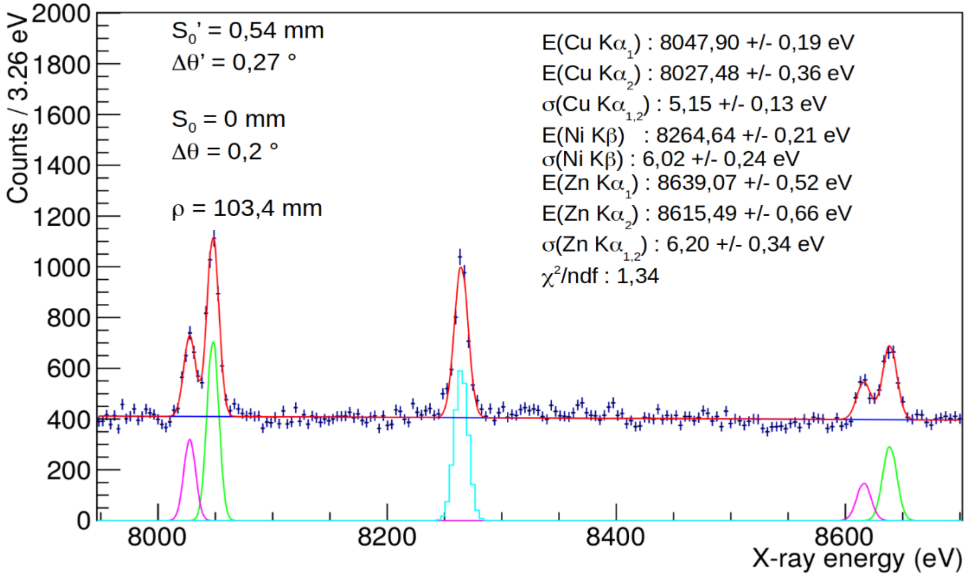

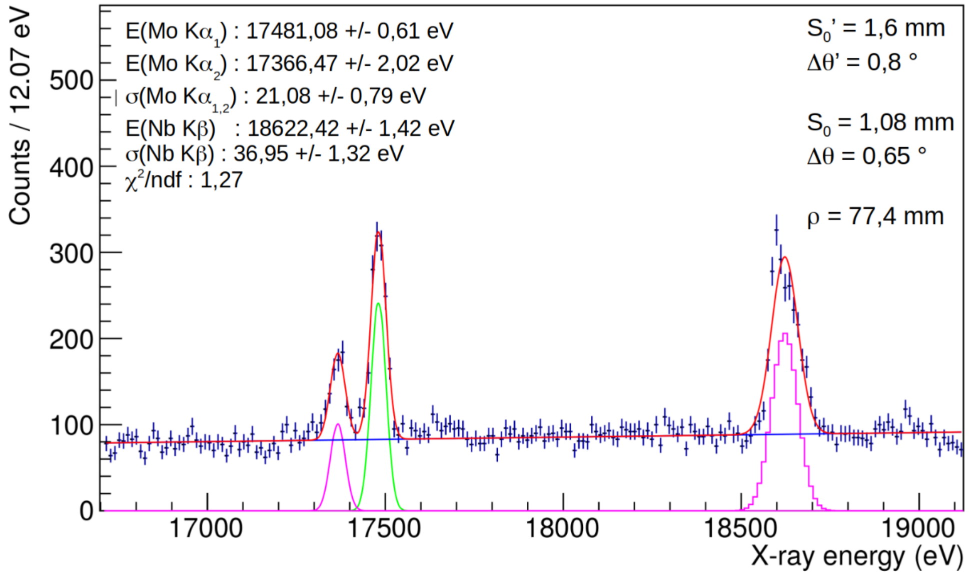

FWHM of few eV with NO COOLING

Energy range (θ_B>5°) between 2-20 keV (n=1) and 6-60 keV (n=2)

Extremely low efficiencies
(solid angle, micrometric sources)

- One-shot large energy range spectra
- Effective source sizes of mm (Bragg) x cm (Vertical) dimensions
- Resolutions still in the "classic" range of Bragg spectrometers

V. De Leo et al., Condensed Matter, 2022, 7,1
A. Scordo et al., PoS PANIC2021 (2022) 195
A. Scordo et al., RAP Conference Proceedings, 6 (2021), 82–86
A. Scordo et al., J. Anal. At. Spectrom., 2021, 36, 2485-2491.
A. Scordo et al., J. Anal. At. Spectrom., 2020, 35, 155–168.
A. Scordo et al., Condensed Matter, 2019, 4, 59.

Extremely high precision kaonic atoms spectroscopy

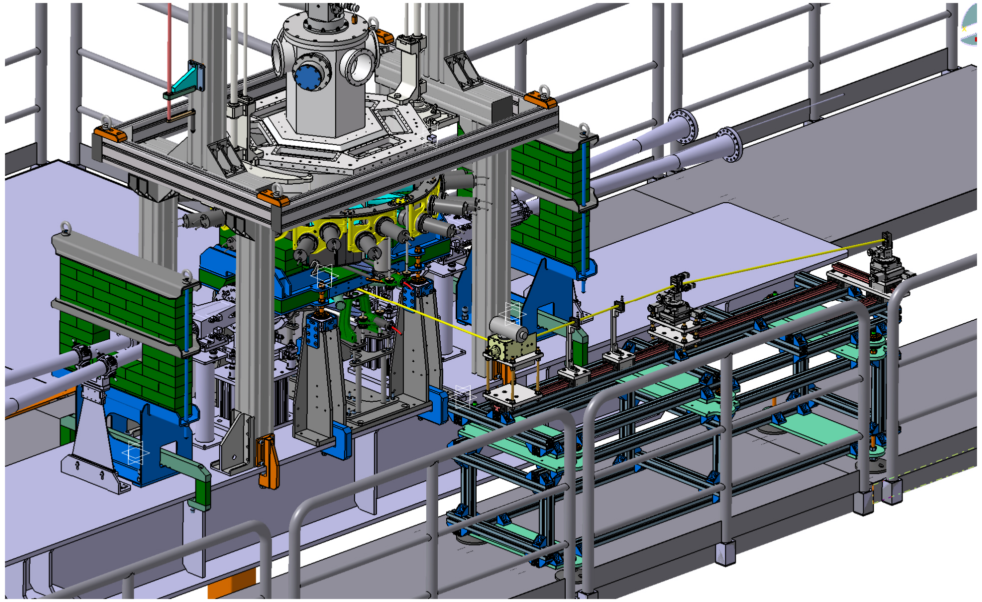

The VOXES spectrometer could also be used to perform exploratory measurements of kaonic atoms in DAΦNE

Resolutions comparable with TES

Agrifood

TRANSPORTABLE AND AGILE SPECTROMETER FOR METAL TRACE IN EDIBLE LIQUIDS : TASTE

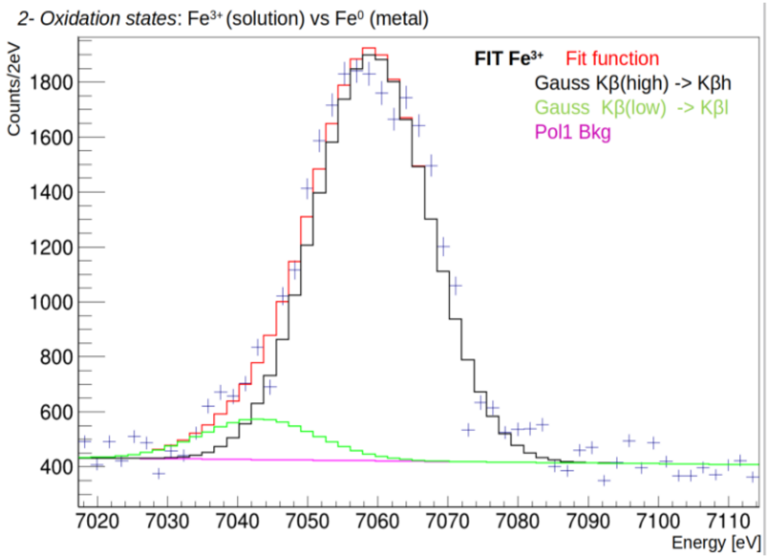

First attempt to use the VOXES spectrometer with liquid samples:

Fe oxidation states in wine browning

C. Fiorini – INFN, PoliMI / M. Porro, XFEL

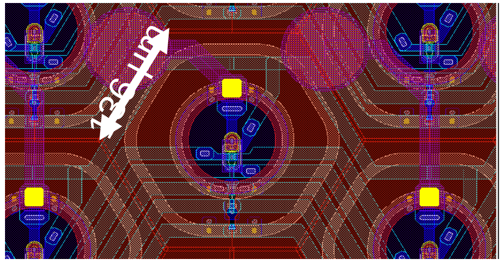

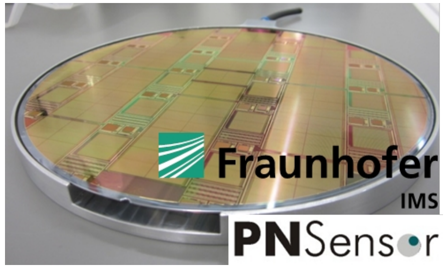

DEPFET Active Pixel

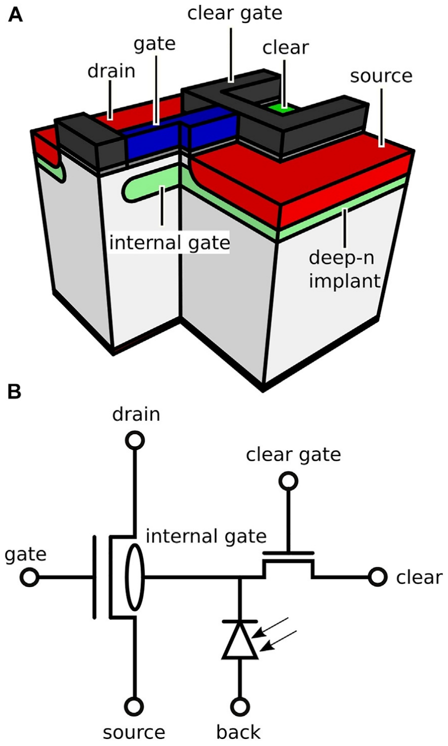

The DEPFET (DEPleted Field Effect Transistor) is an active pixel sensor combining sensor and first amplification stage.
It consists of a MOSFET built on a high resistivity n-doped silicon wafer

The MOSFET consists of source, drain and
external gate.

A deep-n implant below the external gate forms a potential minimum for electrons.

As the device is fully depleted by a thin p + backside contact, charge generated within the bulk, will be collected in the so-called internal gate, increasing the channel conductivity.

By measuring this change the number of collected charge carriers can be deduced.

The current change is either directly measured or a constant current is imprinted on each
channel of the DePFET and the change of the source-potential in this source follower configuration is measured.

Lechner, P.; et al. DEPFET active pixel sensor with non-linear amplification, 2011 IEEE Nuclear Science Symposium Conference Record, 2011, pp. 563-568, doi:10.1109/NSSMIC.2011.6154112.

*Aschauer, S.; et al. First Results on DEPFET Active Pixel Sensors Fabricated in a CMOS Foundry - a Promising Approach for New Detector Development and Scientific Instrumentation.
J. Inst. 2017, 12, P11013–P11013. doi:10.1088/1748-0221/12/11/p11013*

- 100 μA/pixel <u>average</u> DEPFET-bias current
- ***ENC 18 e- rms*** with T_{int} = 50 ns (2.25 MHz), 200 eV/ADU
- Down to **9.8 e- rms** with T_{int} = 300 ns (1.125 MHz operation), 37.3 eV/ADU
- Near room-temperature conditions

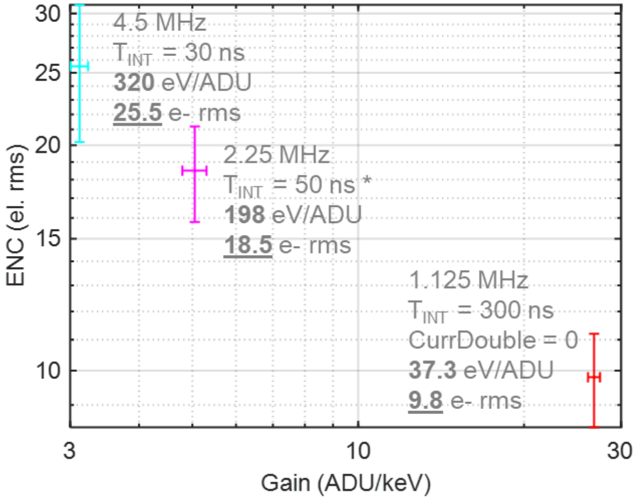

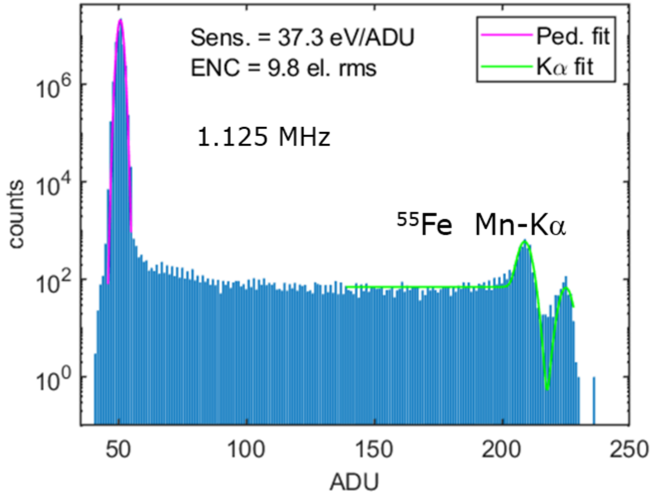

Low ENC enable very low energy imaging (< 1 keV)

DePFET With Signal Compression

tailoring of the internal gates shape to implement a non-linear signal response and provide a larger dynamic range or a drastic increase of the DEPFETs amplification.

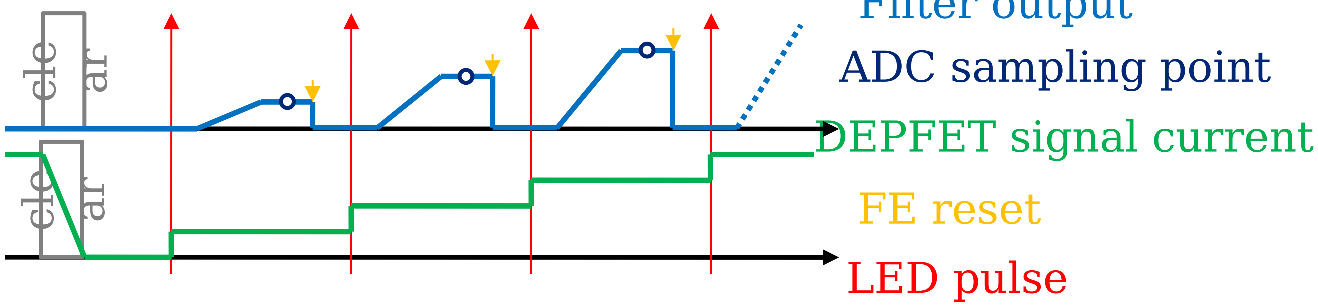

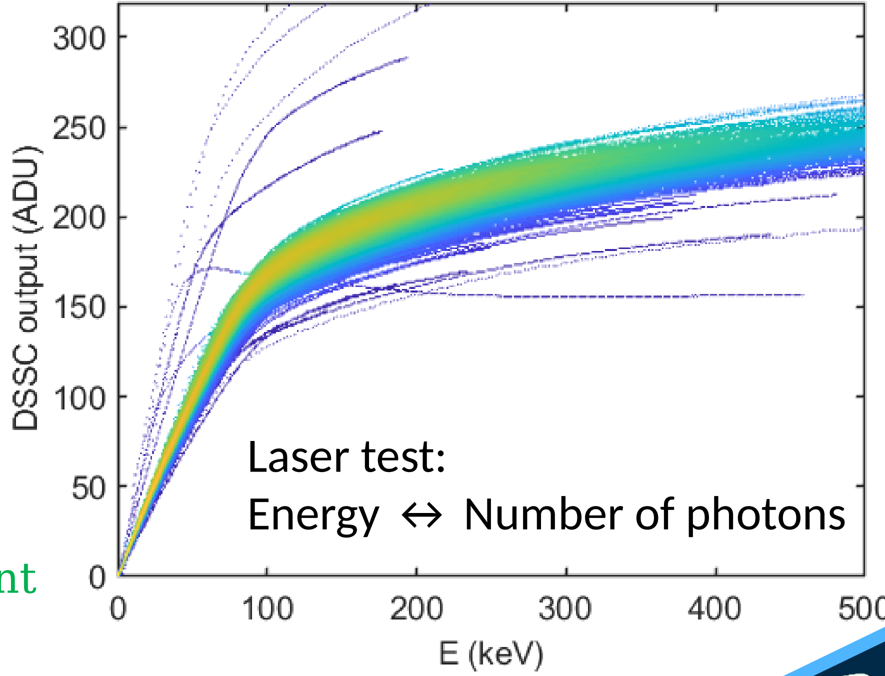

Belle II experiment utilizes DEPFET based matrices for the two innermost layers of its particle tracker

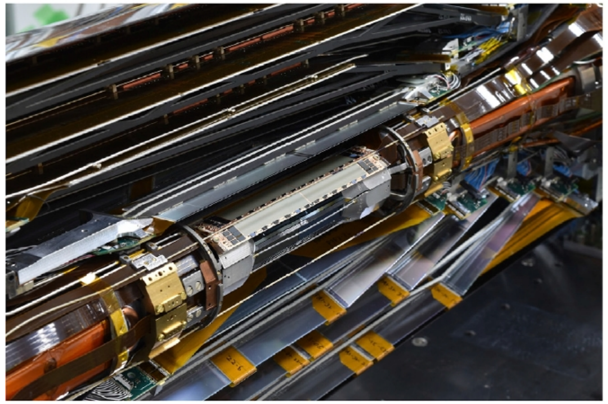

2 layers of pixelated detectors (PXD)

256 × 768 pixels of 55 × 50 μm^2 (inner layer)

85 × 55 μm^2 (outer layer)

The first space born instrument utilizing DePFETs:
Mercury Imaging X-ray Spectrometer (MIXS) aboard the BepiColombo Spacecraft.

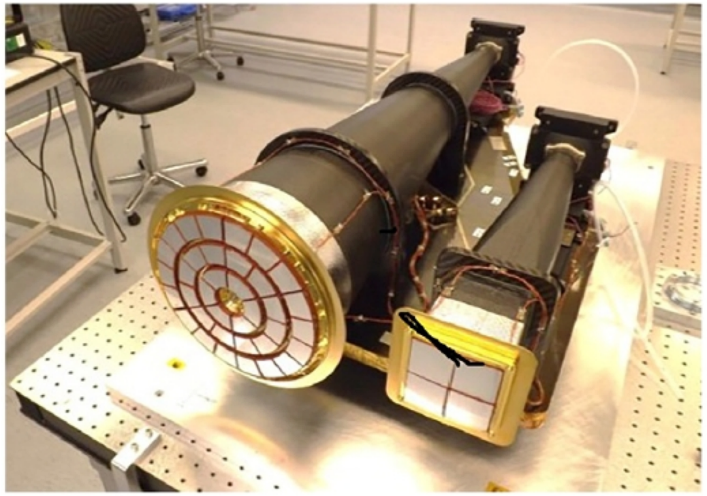

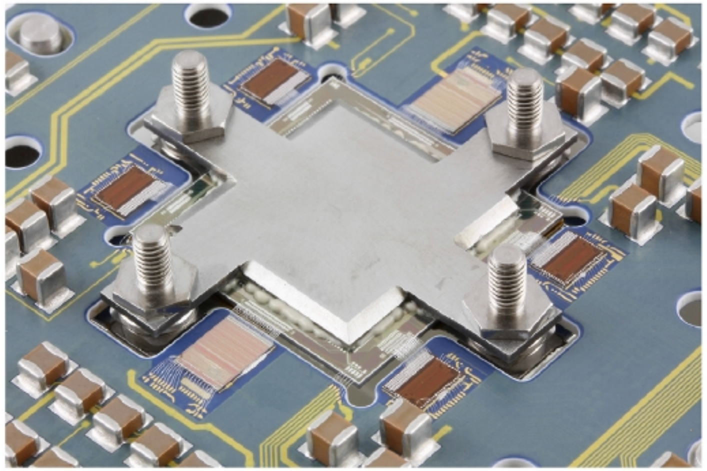

Collimator (MIXS-C) + high resolution telescope (MIXS-T) witha DePFET matrix in their focal plane.

The goal of MIXS is to provide information about the elemental composition of Mercuries surface.

With flight electronics a noise of 7.9 e- was estimated.

The sensor provides near Fano-limited noise over the required energy range from 0.5 keV up to 7 keV.

The planned arrival of BepiColombo at Mercury is in 2025

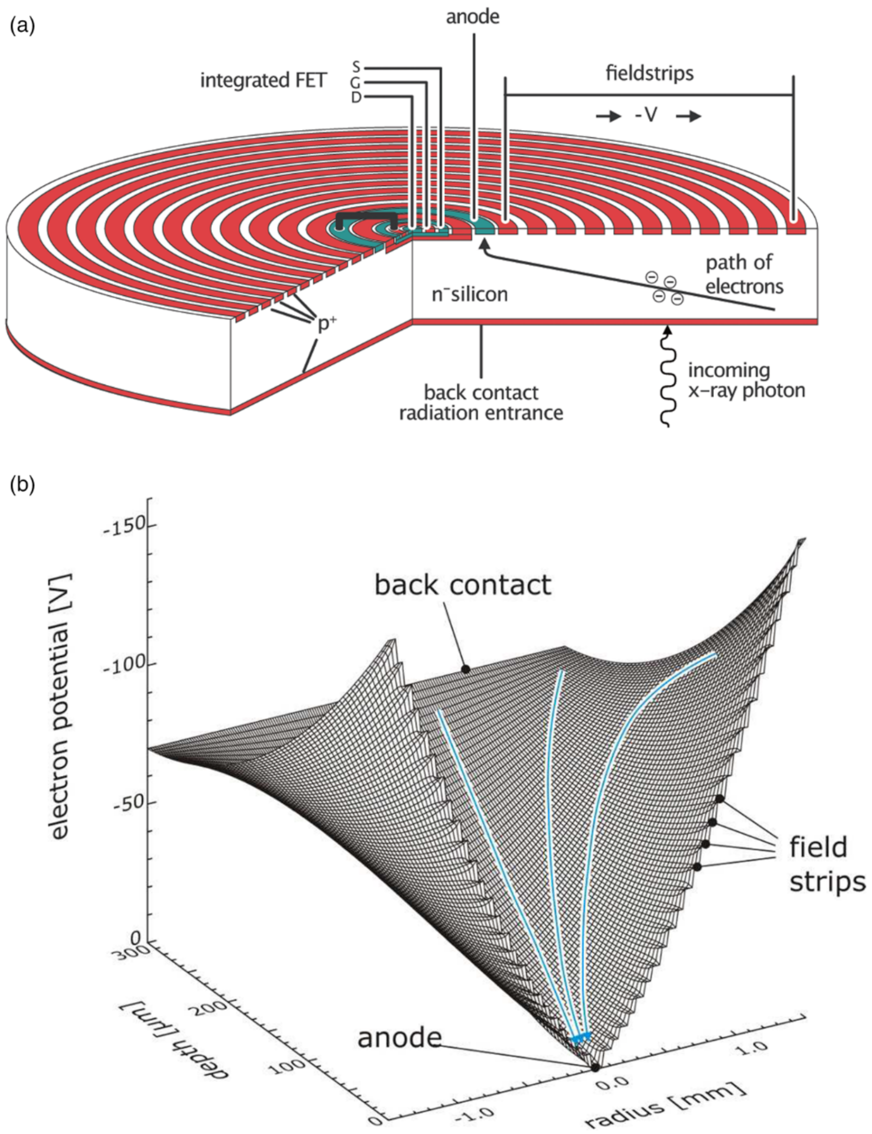

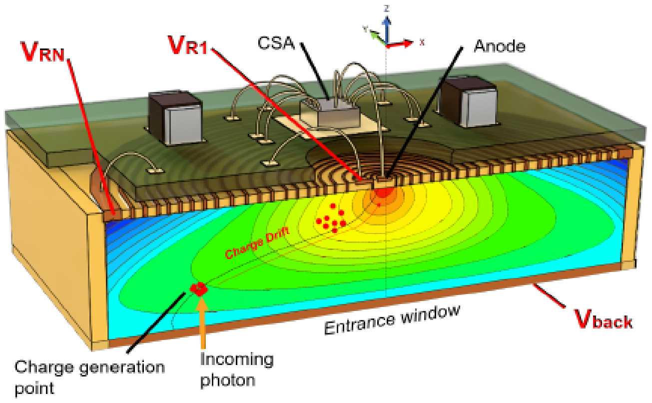

p+ n- junction based devices

Central anode to collect the electrons

Several rings with increasing potential to create funnel-like potential and enhance e- drift

Thick SDD: extending the working range

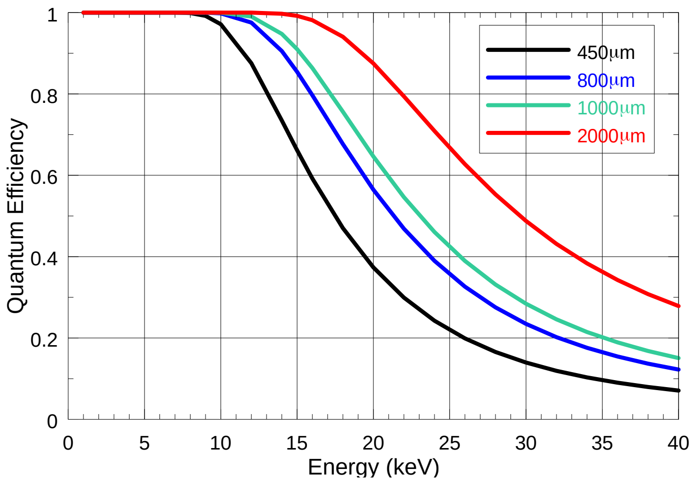

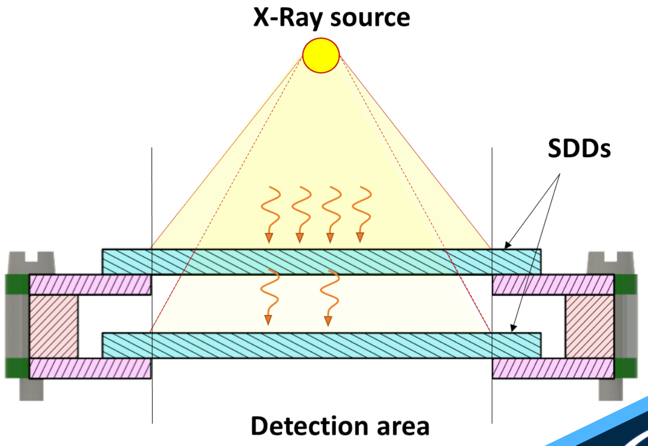

C. Fiorini – INFN, PoliMI

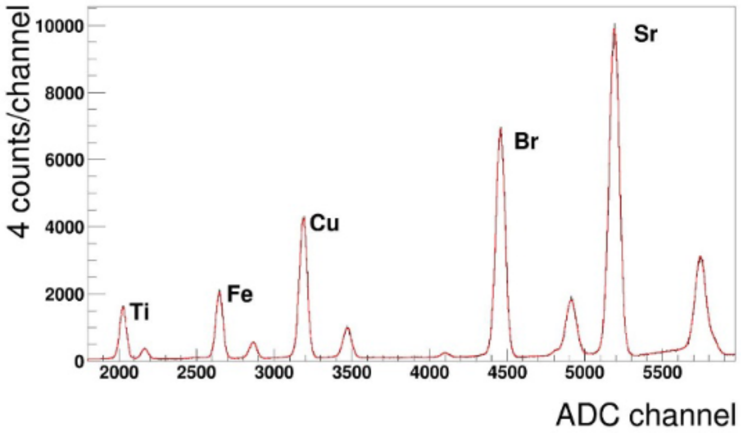

$$G(x) = H_G \cdot e^{\frac{-(x-x_0)^2}{2\sigma^2}}$$

$$T(x) = \frac{H_T}{2\beta\sigma} \cdot e^{\frac{x-x_0}{\beta\sigma}+\frac{1}{2\beta^2}} \cdot \mathrm{erfc}\left(\frac{x-x_0}{\sqrt{2}\sigma}+\frac{1}{\sqrt{2}\beta}\right)$$

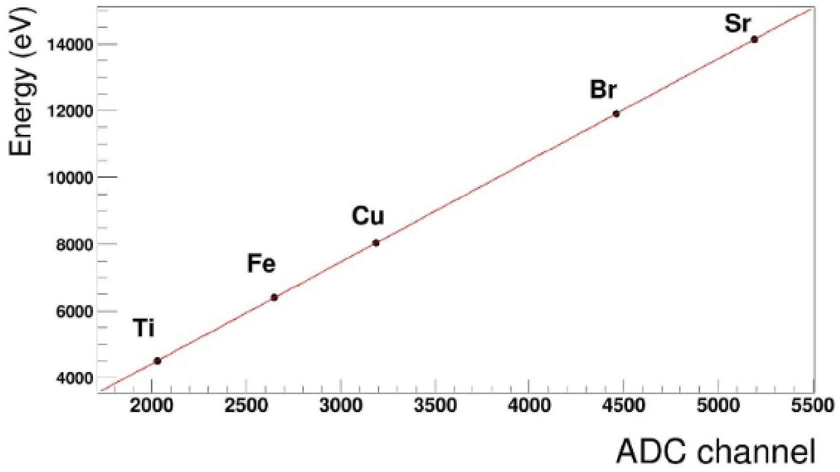

Linearity of $\Delta E/E < 10^{-3}$

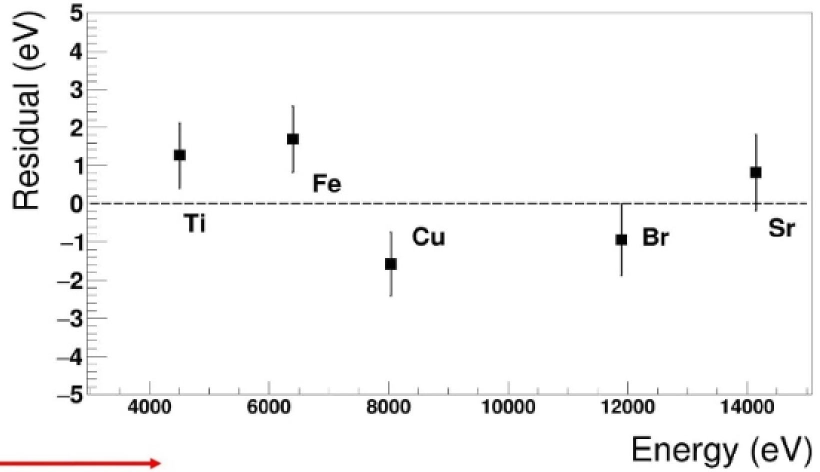

G(x) represents the fluorescence X-rays,
T(x) represents the events with charge-loss

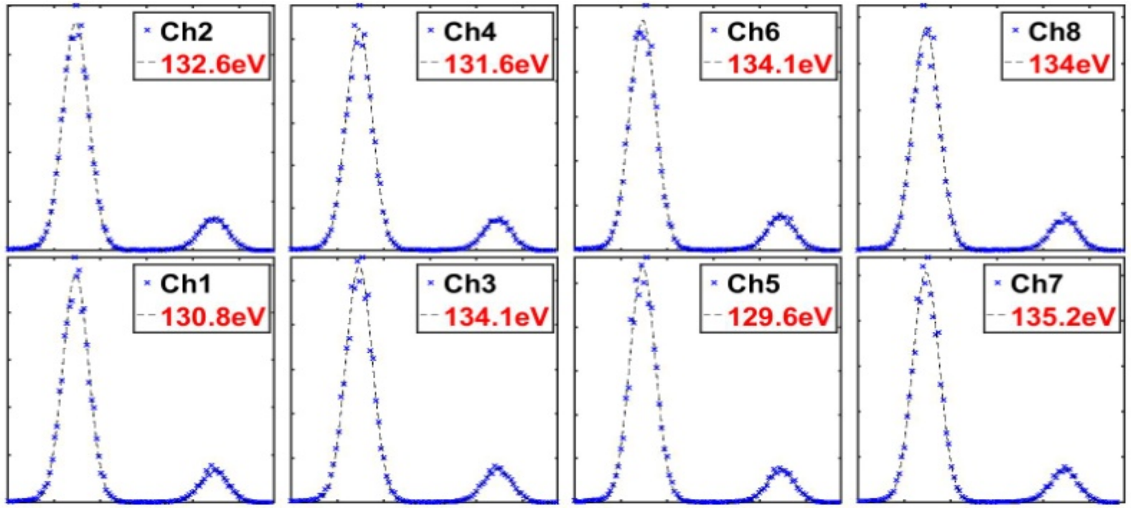

^{55}Fe X-ray spectra measured with Siddharta SDD array read out by SFERA with a 4 μs shaper peaking time at a temperature of -30 °C.

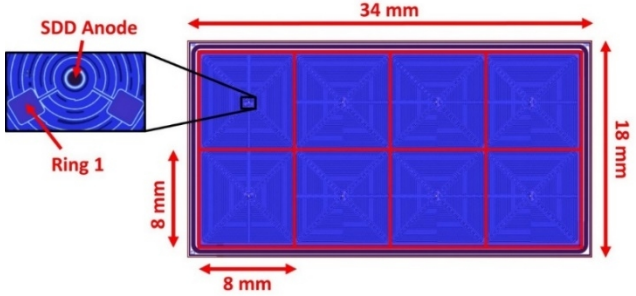

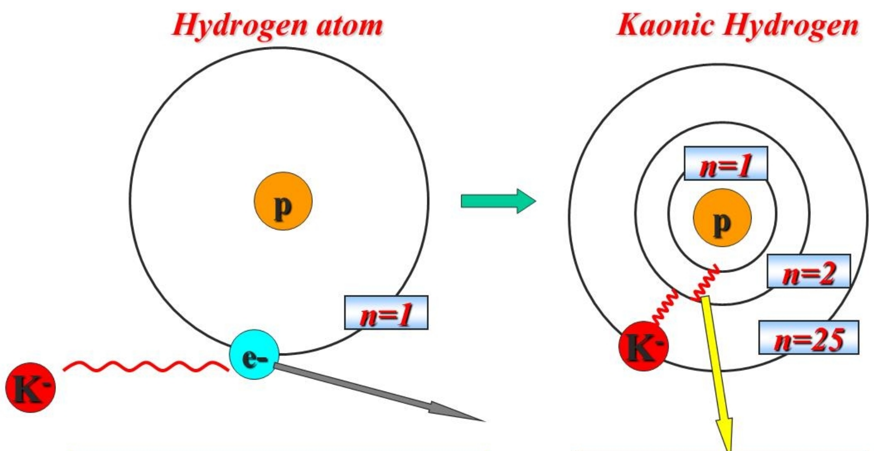

$$\varepsilon = \left|E^{measured}_{2p-1s}\right| - \left|E^{e.m.}_{2p-1s}\right|$$

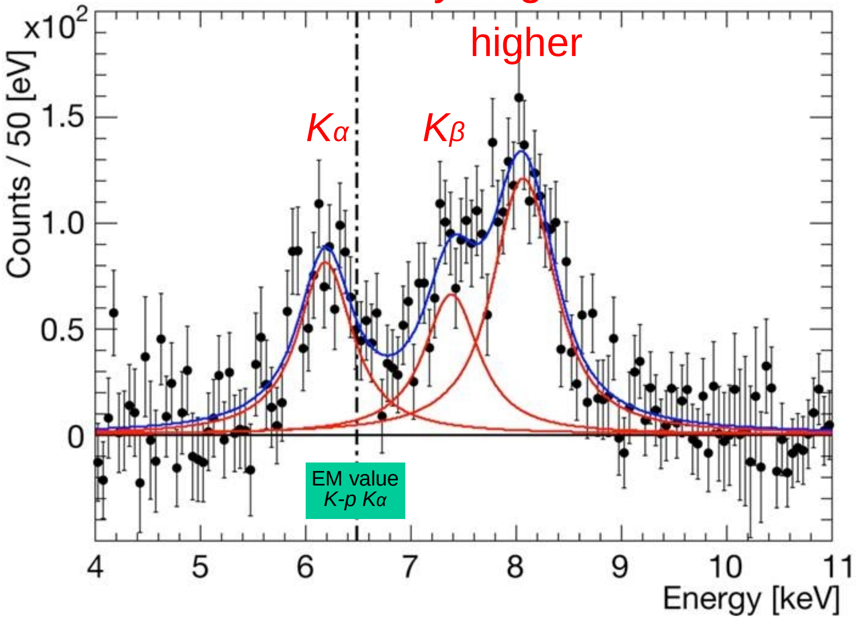

Strong interaction studies al low energy through **precise X-ray spectroscopy measurements** of Kaonic atoms transitions

Most precise measurement of 1s level shift and width in KH

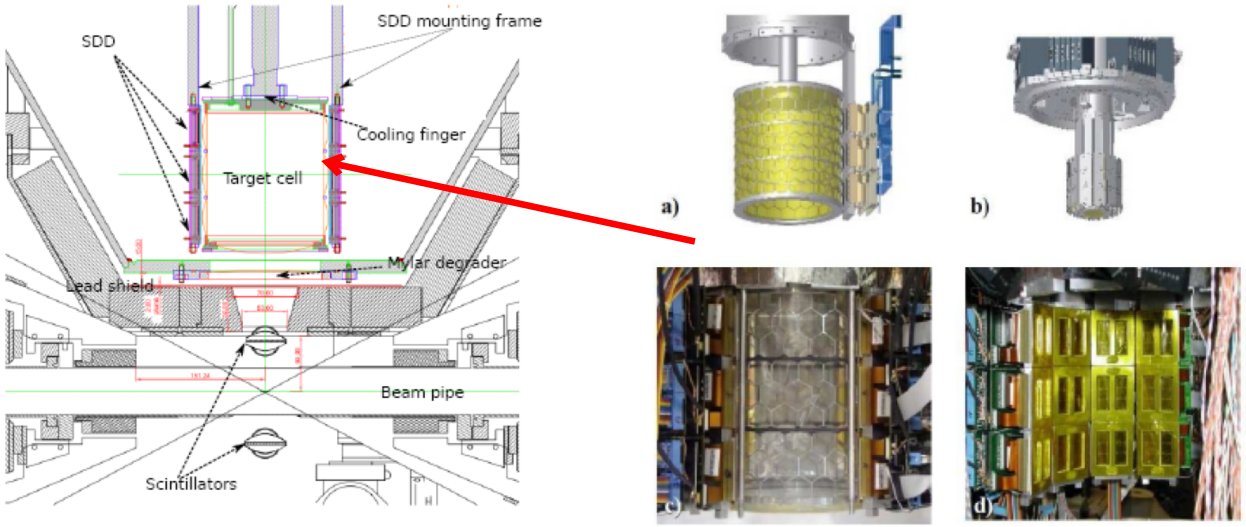

$$\epsilon_{1s} = -283 \pm 36(\mathrm{stat}) \pm 6(\mathrm{syst})\ \mathrm{eV}$$

$$\text{and} \quad \Gamma_{1s} = 541 \pm 89(\mathrm{stat}) \pm 22(\mathrm{syst})\ \mathrm{eV},$$

SIDDHARTA Collaboration / Physics Letters B 704 (2011) 113–117

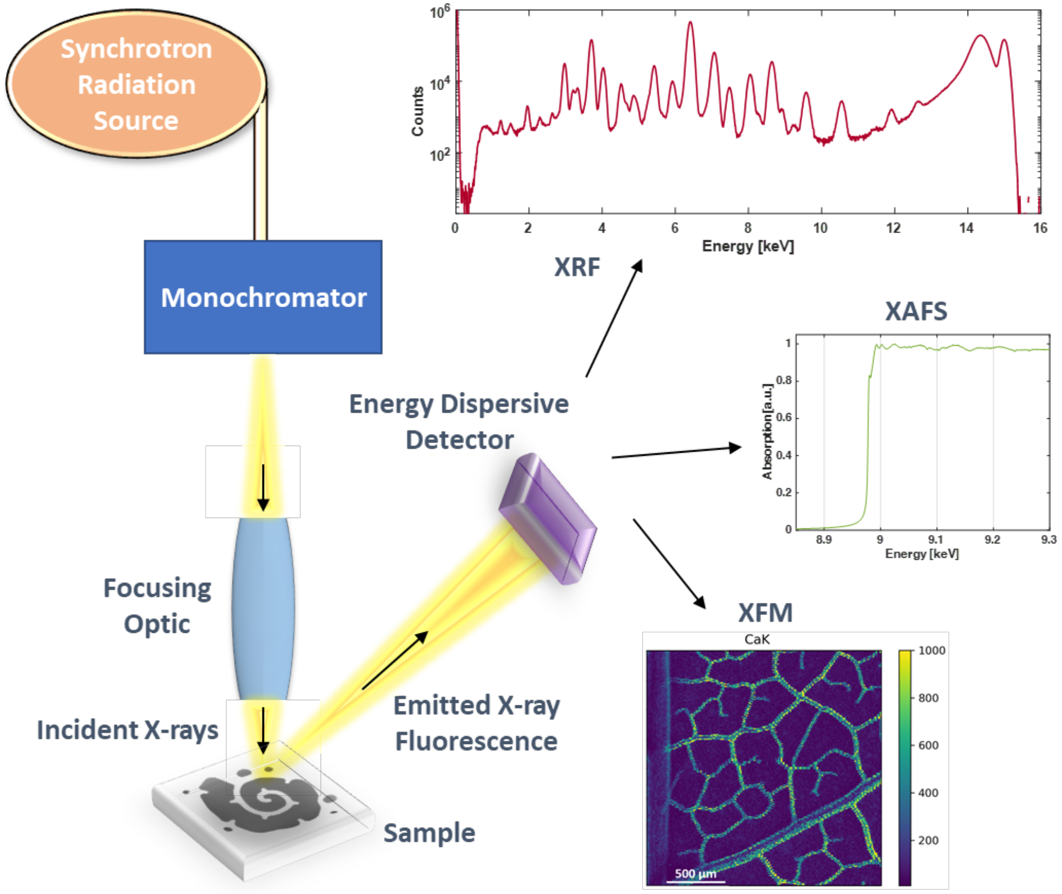

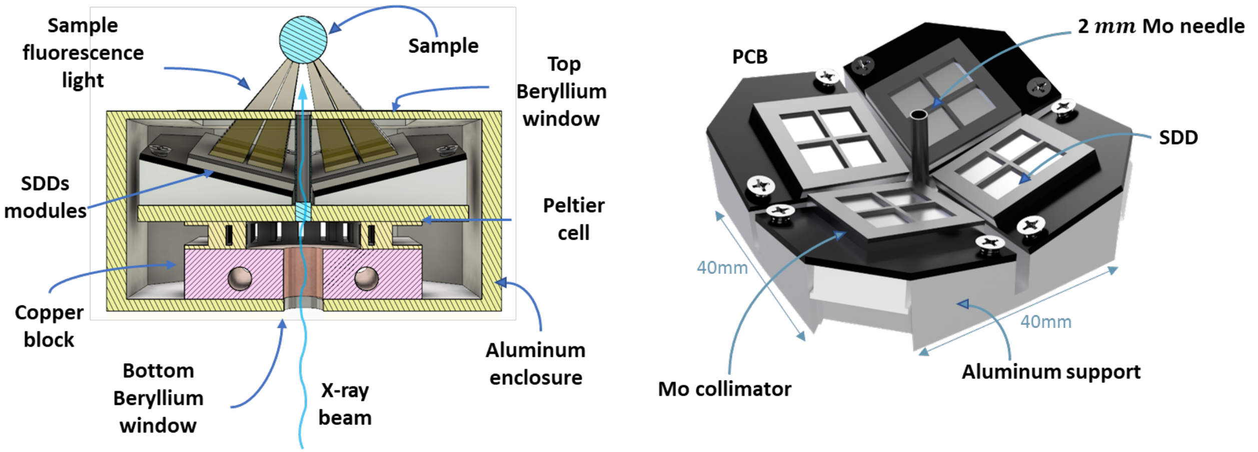

(ASCANIO X-ray detector)

TRISTAN Detector

- ~3500 total channels
- 100kcps per channel

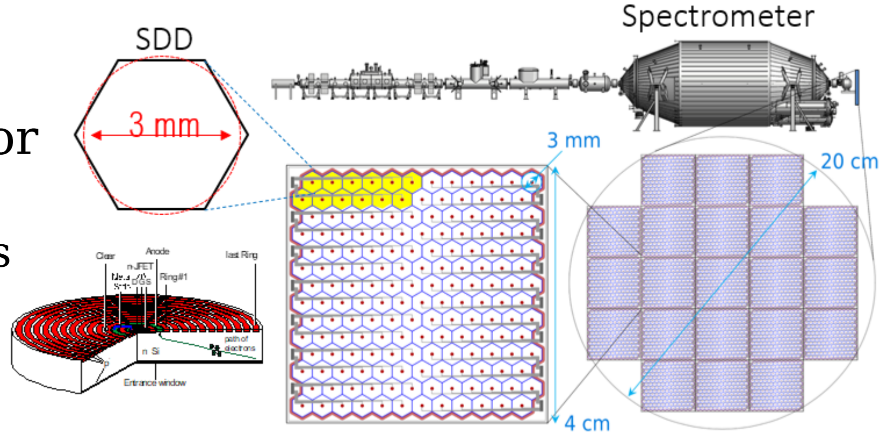

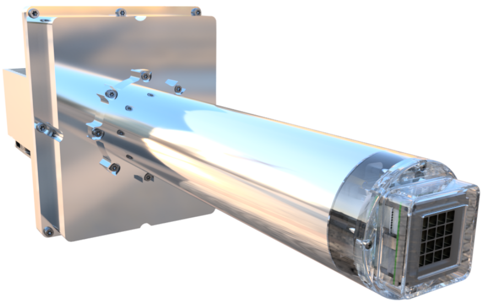

(ARDESIA X-ray Spectrometer)

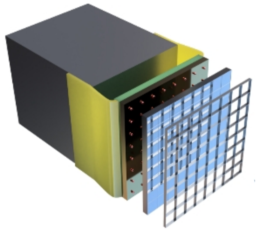

SCARLET Detector

Pixelated SDD bump-bonded to the readout ASIC

22

A. Vacchi, Trieste INFN,
G. Pepponi FBK

RESEARCH DRIFT FOR SOFT X-RAYS redSoX

INFN, INAF, FBK, INAF, ASI, EU, ESA

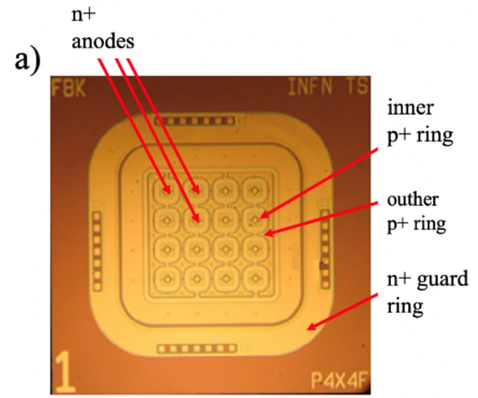

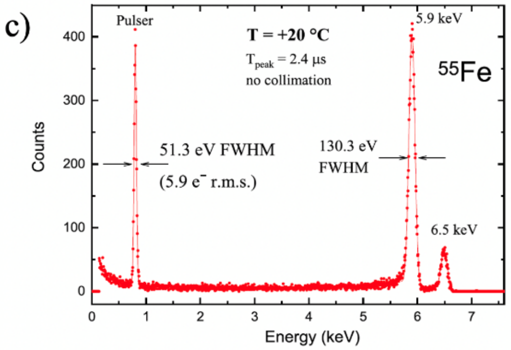

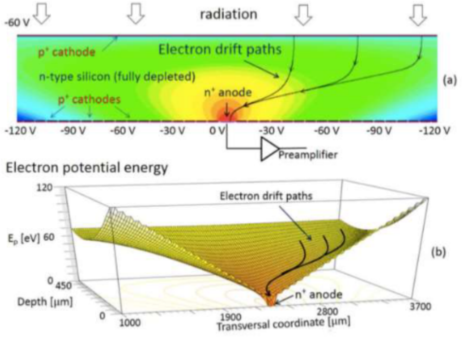

PIXDD: Drift Detectors brought to pixel levels ⇒ Extremely low noise

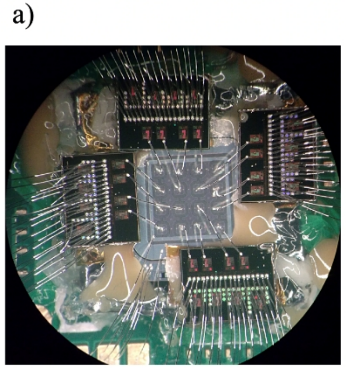

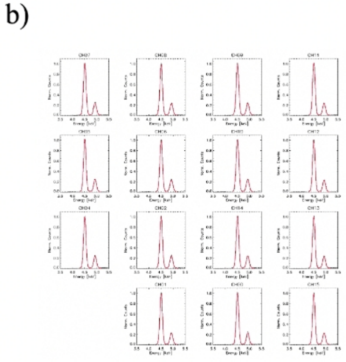

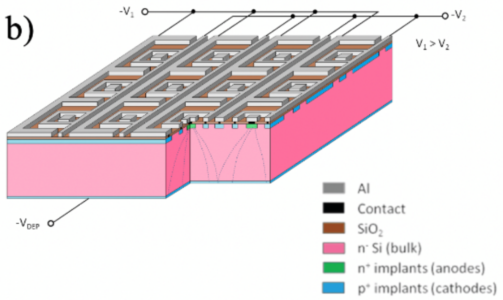

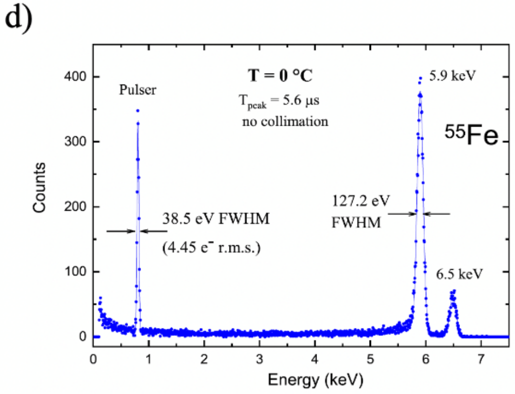

FWHM close to Fano limit obtained AT ROOM TEMPERATURE

PIXDD pixel SDD advanced FBK technology room temperature operating PixDD+RIGEL proposed for the LAMP mission (China)

500x500 μm

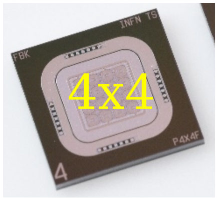

300x300 μm

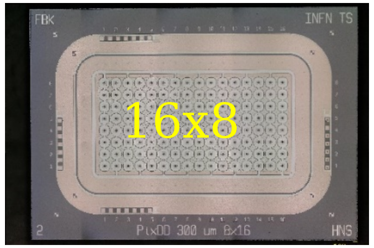

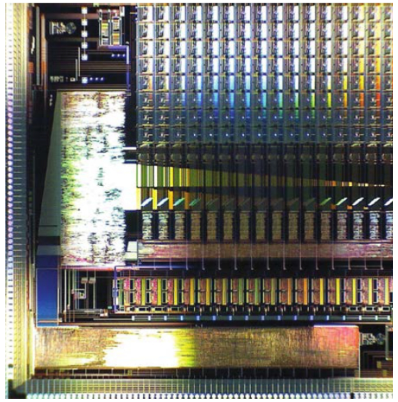

Electronics:
RIGEL SIRIO chip
PoliMi

(bump-bonded)

300x300 μm

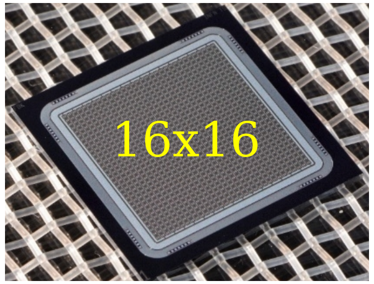

zero edge for tiling advanced study by FBK

Large Area Silicon Drift Detectors (SDD) – From ALICE central tracking to Large Area Detector LAD for the eXTP mission; high-throughput, spectral-timing instrument

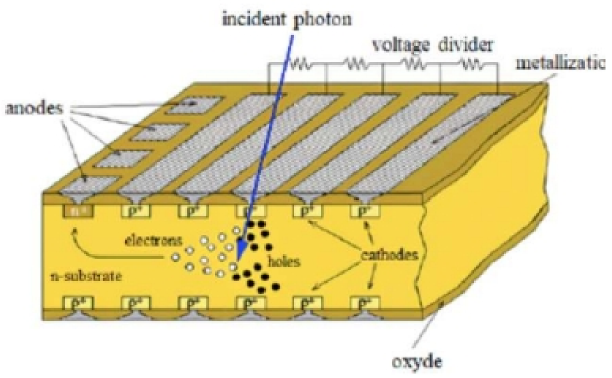

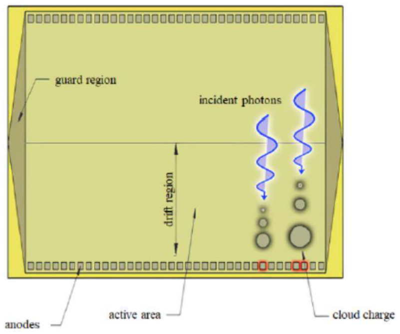

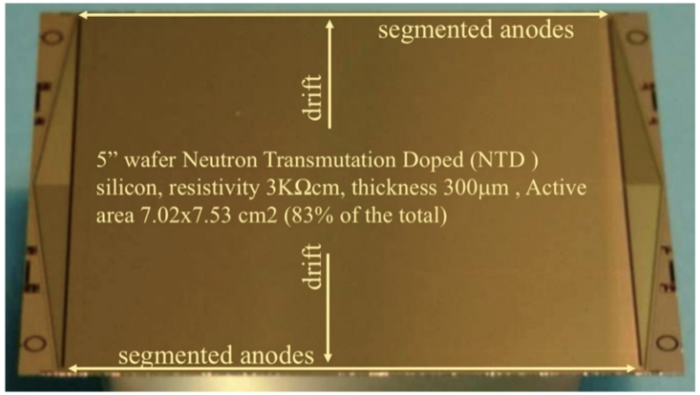

Science case: Dense matter, Accretion in strong field gravity, Strong magnetism and Observatory science (GRB measurements)

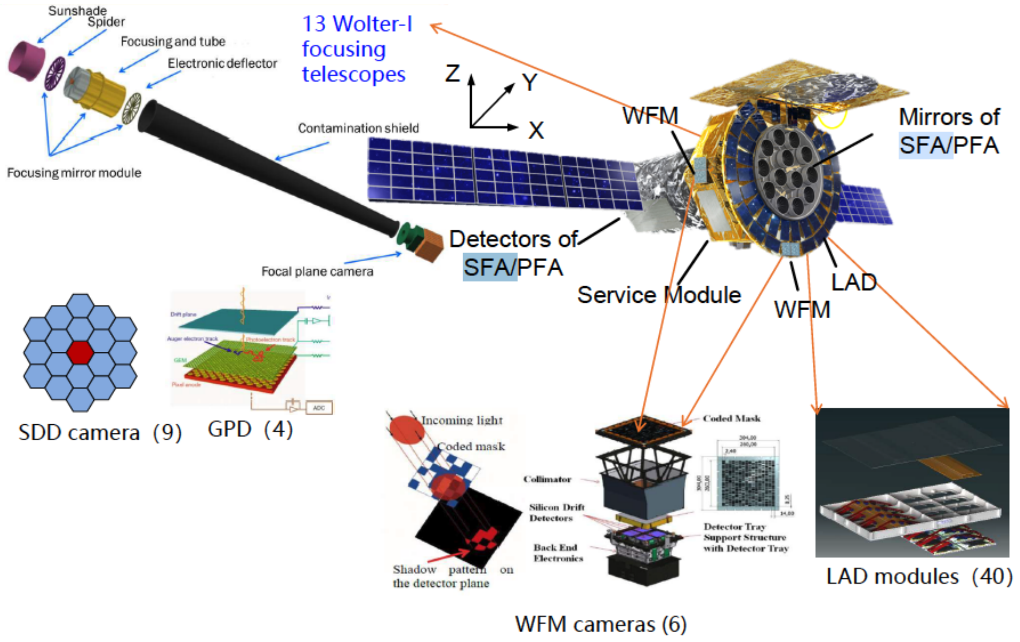

Table 1 The main features of the LAD instrument

Parameter	Value
Energy Range	2-30 keV nominal 2-80 keV extended
Effective Area	>1.3 m² @ 2 keV >3 m² @ 8 keV >1.5 m² @ 30 keV
Energy Resolution	<260 eV FWHM @ 6 keV (all events)
Field of View	<65 arcmin FWHM
Field of Regard	>50%
Time Resolution	10 µs
Absolute Time Accuracy	2 µs
Dead Time	<1% @1Crab
Maximum Flux (sustained)	>1 Crab
Maximum Flux (time-limited)	>15 Crab (300 minutes)
Total Mass	571 kg CBE+DMM
Total Power	769 W CBE+DMM
Telemetry	1 Mbps (typical, for a 250 mCrab source)

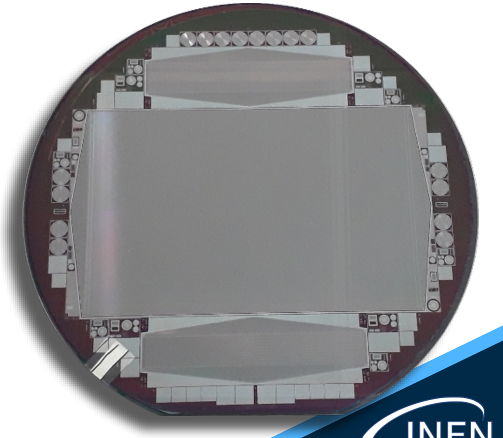

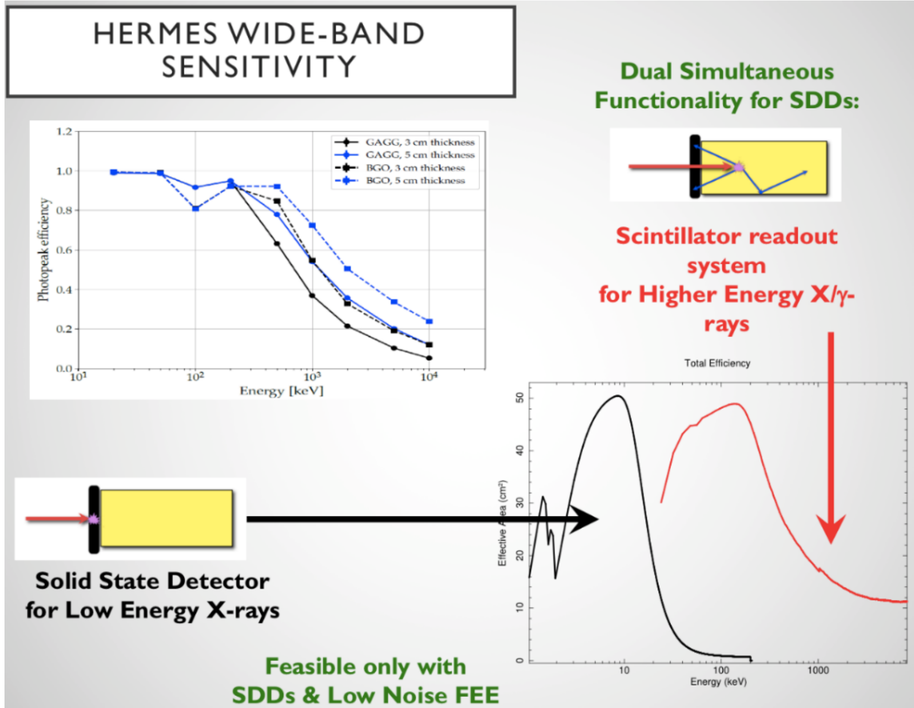

Silicon Drift Detetors coupled to scintillators (SDD) - project HERMES: A costellation of nano-satellites for high energy astrophysics and fundamental physics reseach

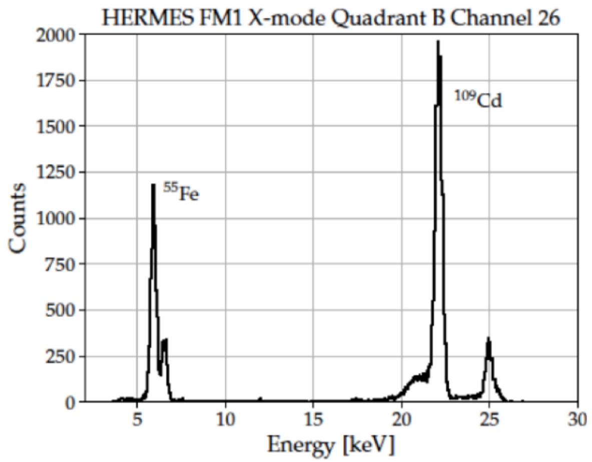

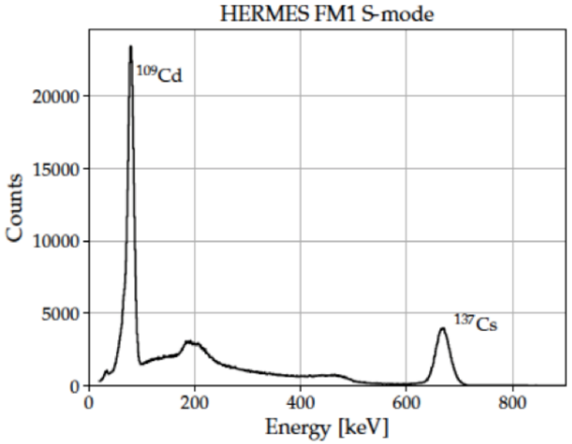

Nano-satellites precursors for future missions

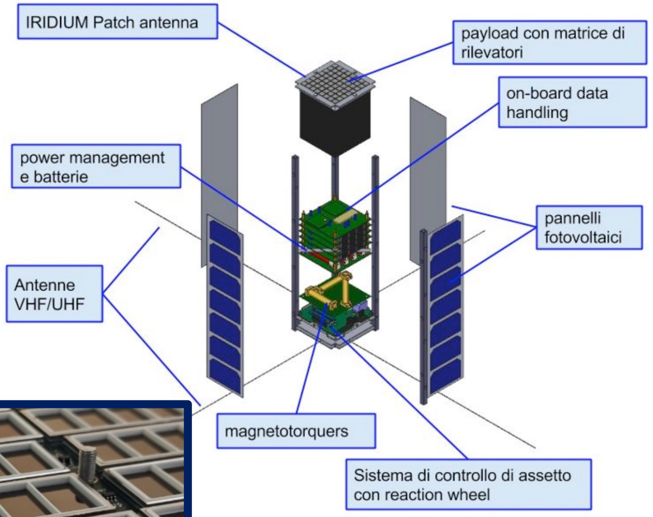

Array size	42.4×42.4 mm^2
Si thickness	450 μm
# of SDDs	64
SDD pitch (n side)	5×5 mm^2
Single SDD active area for scintillator (p side)	4.5×4.5 mm^2
Metal grid between single SDD (p side)	0.5 mm wide
Typical polarization voltage (one connection)	–150 to –200 V
Typical return voltage (one connection/SDD)	–12 to –20 V
Single SDD capacitance	50 fF (typical)
Single SDD dark current (typical @ T= 20 °C)	50 pA (typical)
Optical spectral response	350 – 1000 nm (typical)
Quantum efficiency (@ 560 nm)	> 80 %

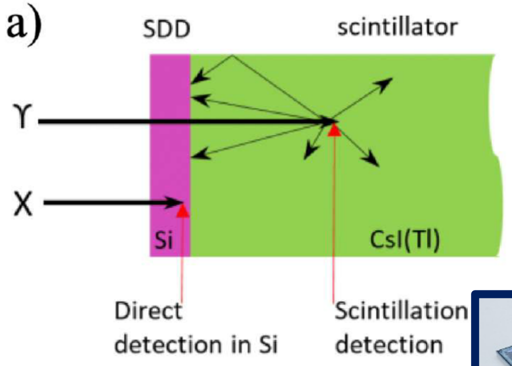

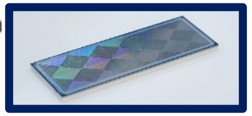

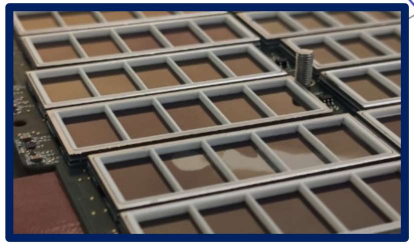

G. Pepponi, FBK

Compact/portable XRF / XRD instruments for material analysis e.g. cultural heritage studies / mineralogy

'Spectroscopic' strip/pixel detectors (FBK/PoliMi)

- Paired-X (strip) XRD+XRF

Core of the project are:

- the Paired-X detector: an Energy dispersive Strip Detector
- algorithm and software to analyze energy/angle intensity maps

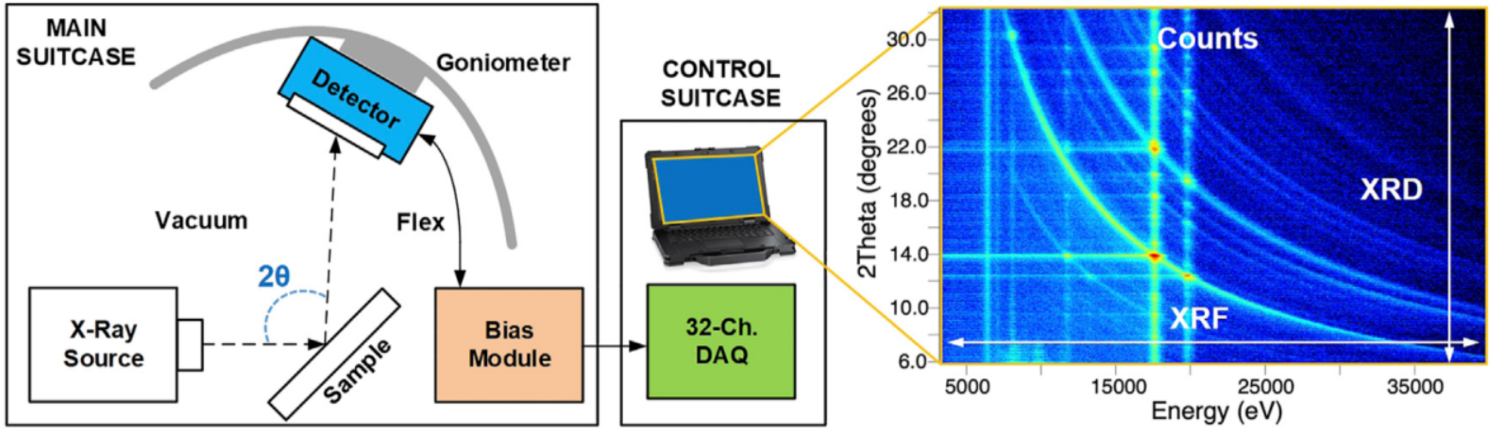

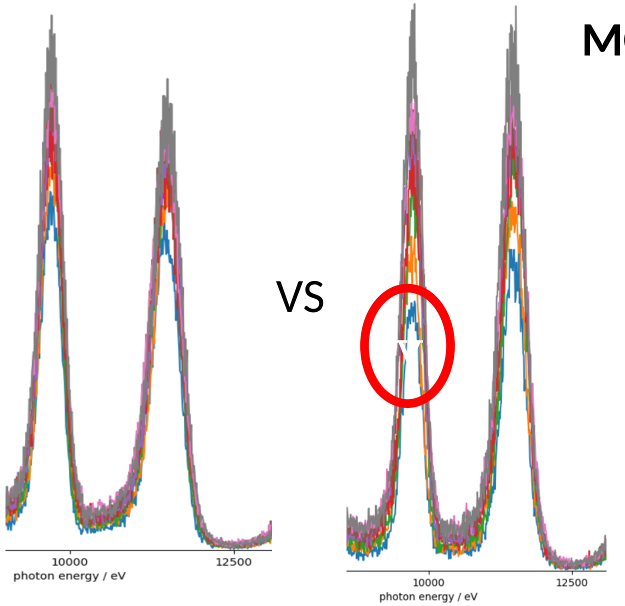

Au Lαβ and Lβ in bulk Au

Au covered by an Al film

MCU based read-out

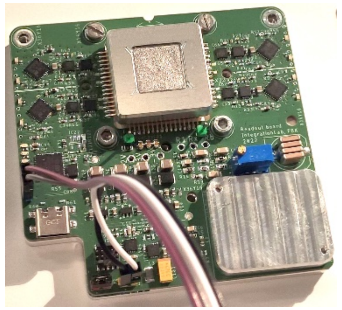

On board:
Power control
8-channels linear SDD Analog filters 12-bit ADC
~4MHz 32-bit MCU USB-communication

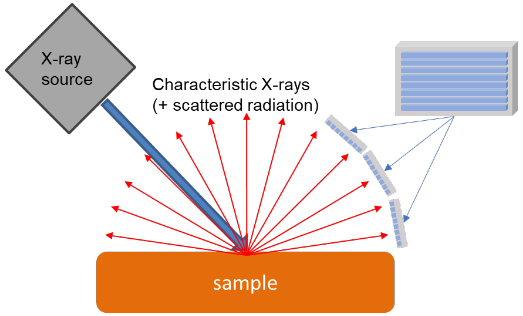

XRF is isotropic but: absorption combined with different path lengths at different angles gives an energy dependent intensity modulation which can carry information especially in stratified materials

Note!
decrease of the Au Lα line

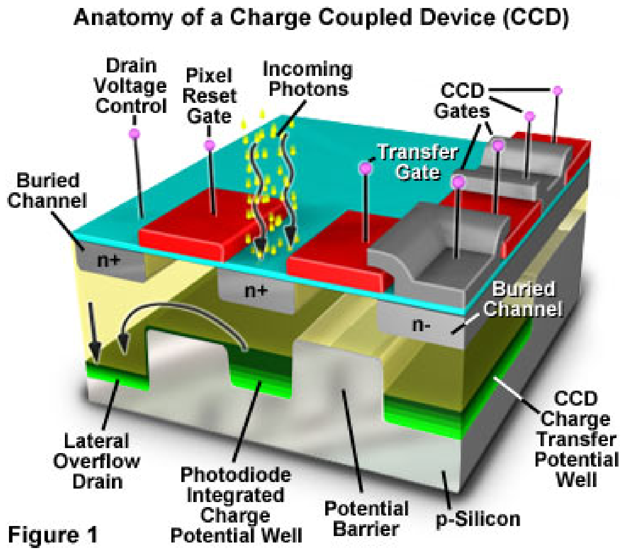

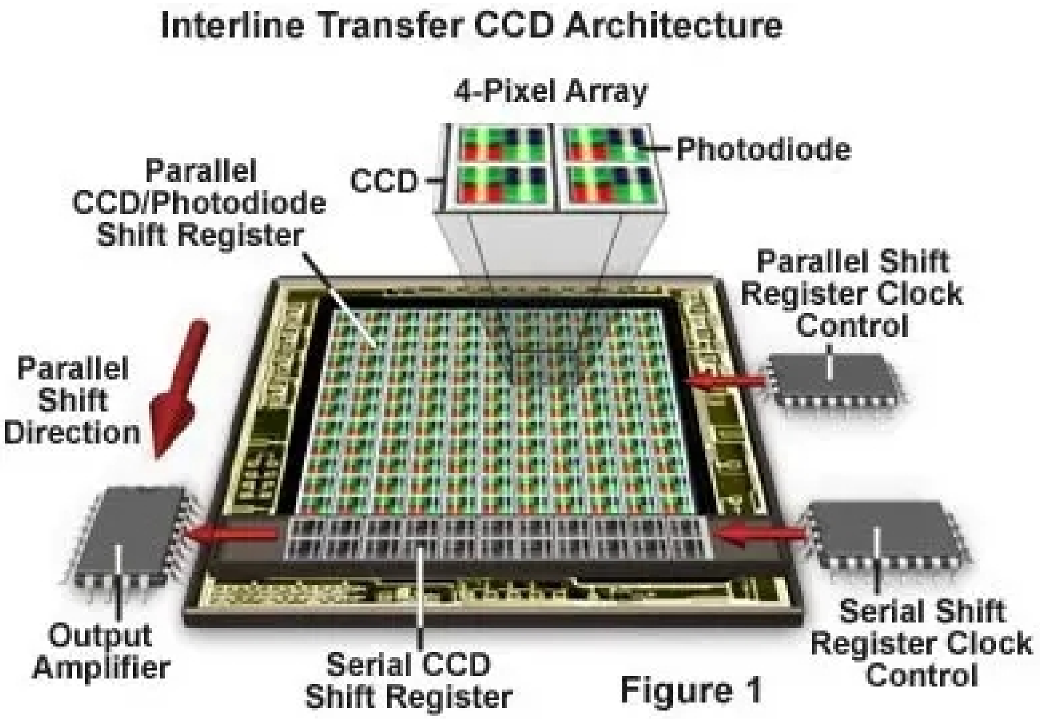

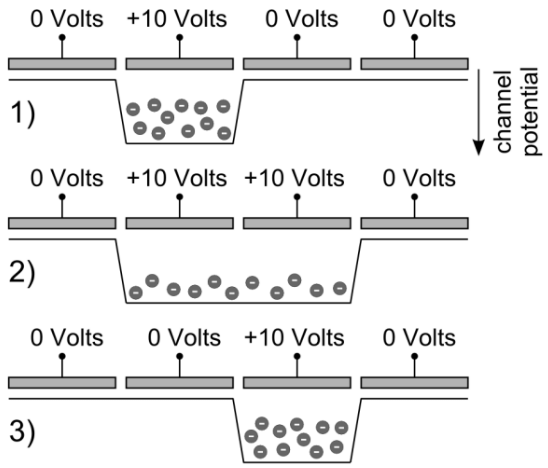

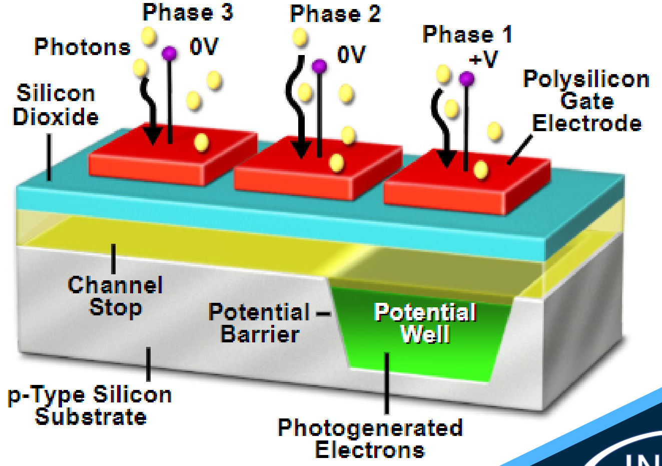

Pixelated detectors for a wide energy range

Cumbersome and slow readout :
Charge Transfer with phase clocking

Ideal for low rates applications

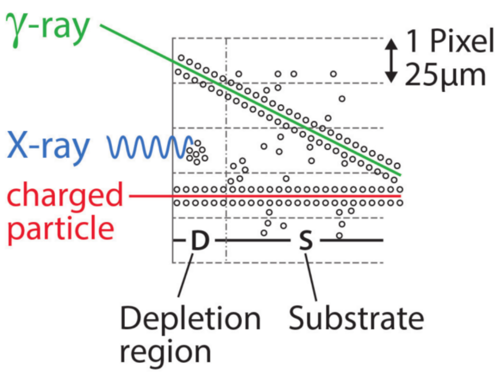

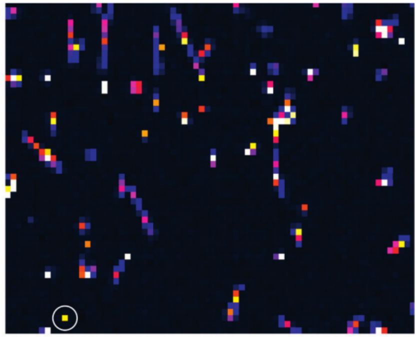

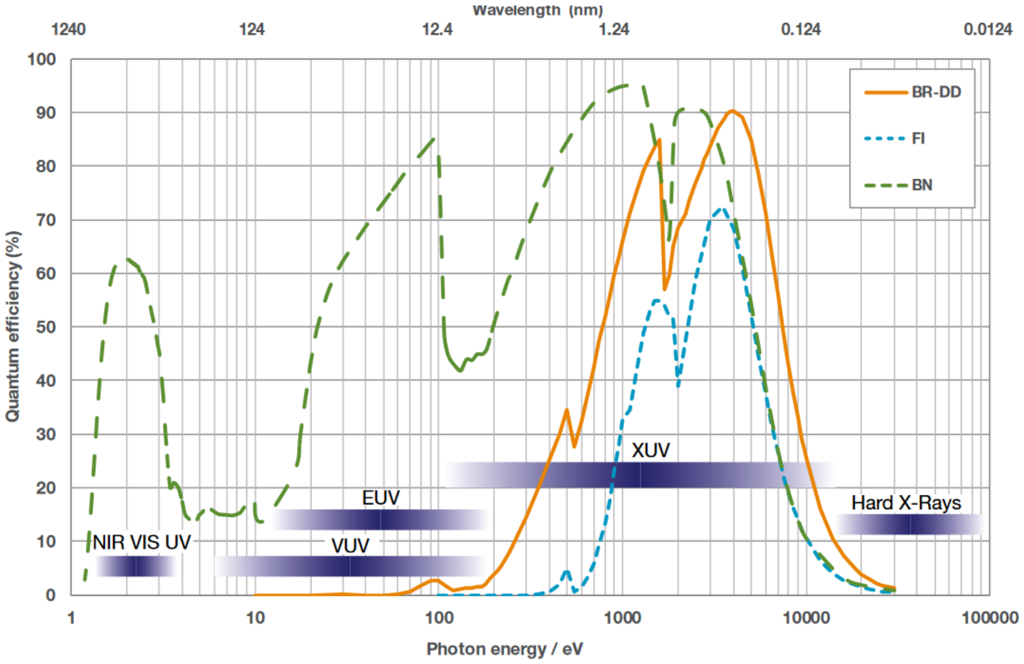

Back/Front Illumination and Deep Depletion are used to tune the energy range

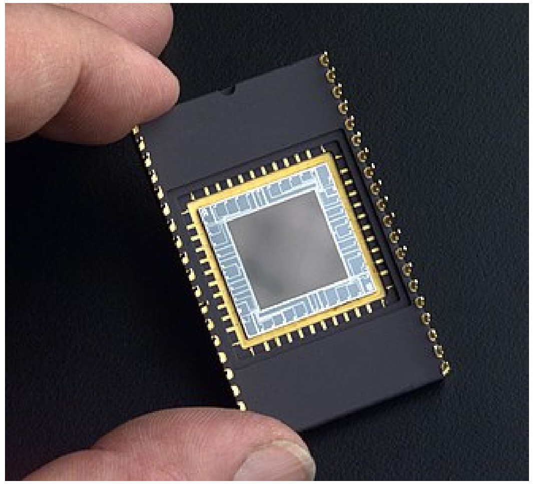

Few microns pixels

Pixel readout rates up to MHz

Dark currents < 10^{-3} e^{-}/pixel/sec.

(Rate dependent) readout noise < 20 e^{-}

Linearity better than 99%

M. Iliescu, LNF

Structure Probing by Holographic Imaging at Nanometer scale with X-ray lasers (SPHINX)

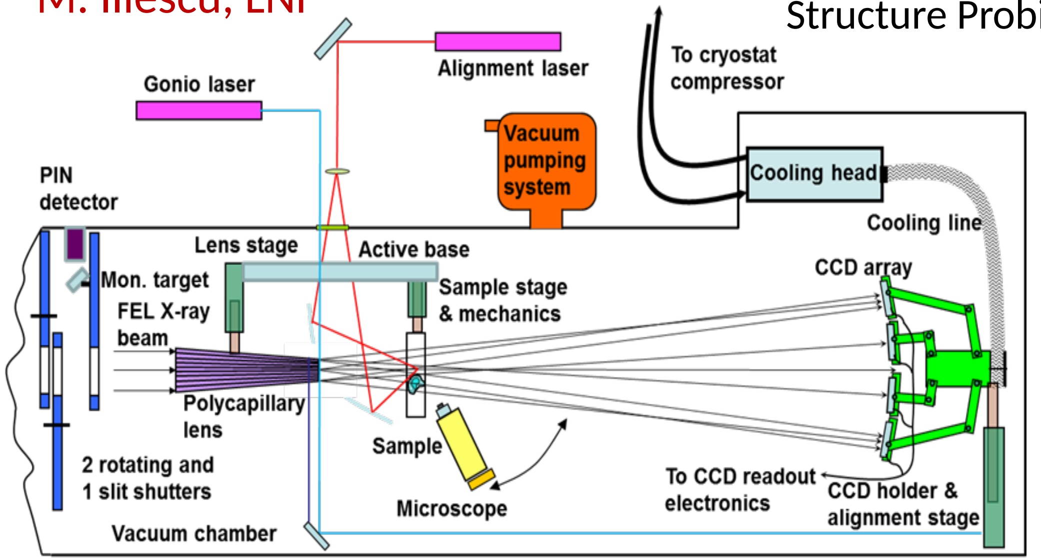

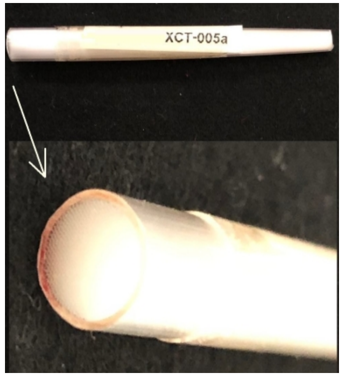

SPHINX aims producing an X-ray phase-contrast holography system for imaging microscopic samples and their internal parts with nanometer resolution, using a combination of polycapillary lenses, large X-Ray CCD arrays and XFEL sources. The proposed configuration allows beam splitting, focusing, magnification and refractive diffraction in the keV range.

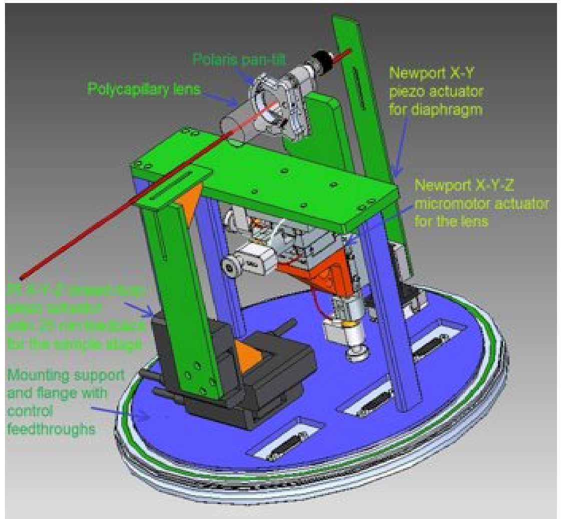

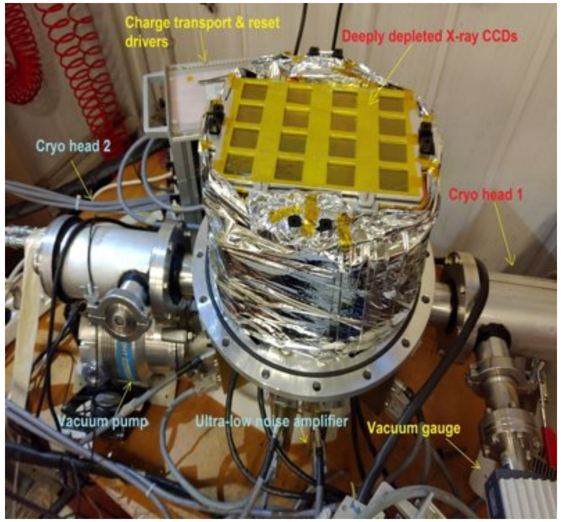

Status at the end of financed period :

1. Full design finalized; production in advanced phase.
2. First X-ray optics delivered, synchrotron tests in preparation (waiting for mobility opening).
3. DAQ and slow control software completed.
4. MC code in advanced phase; reconstruction program work initiated
5. Calibration system under development

https://phase1.attract-eu.com/wp-content/uploads/2019/05/SPHYNX.pdf

M. Bettelli, IMEM-CNR, Parma

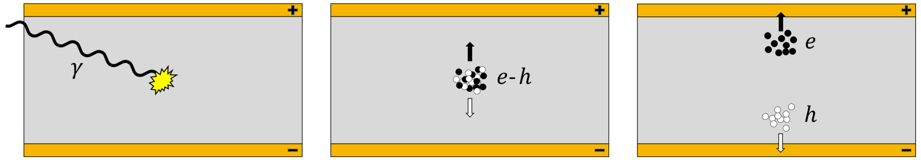

- Sample A: 4x4x3 mm^3

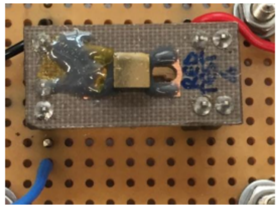

Fig. 2: Sample A

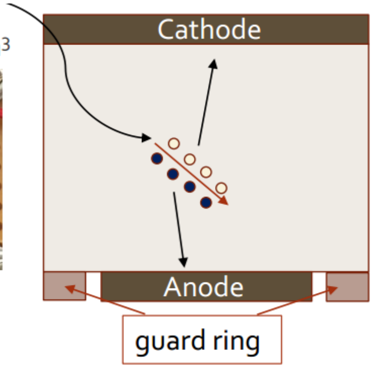

Fig. 5: Configuration with guard ring

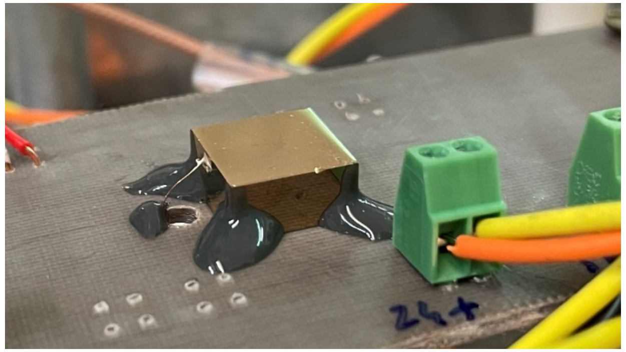

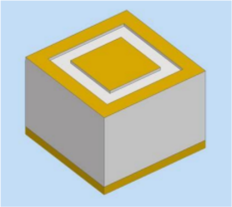

Fig. 6: Structure of Sample A [8]

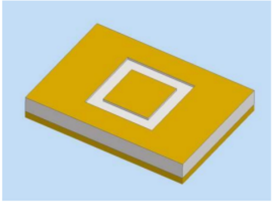

Fig. 7: Structure of Sample B [8]

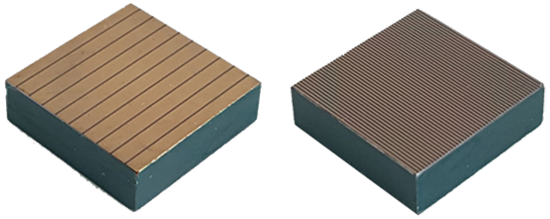

20x20x6 mm

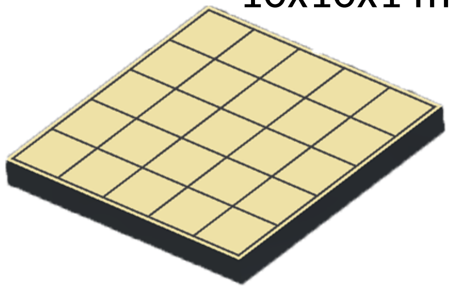

10x10x1 mm

Compound	Si	Ge	GaAs	CZT	CdTe
Mean atomic number	14	32	32	**49.1**	50
Bandgap (eV)	1.12	0.66	1.42	**1.57**	1.5
electrons (cm^2/V)	2-5	5	10^{-4}	**10^{-2}**	10^{-3}
holes (cm^2/V)	1-2	2	10^{-5}	**$3\ 10^{-5}$**	$5\ 10^{-4}$
Resistivity (Ωcm)	$2.3\ 10^{5}$	47	10^{8}	**$5\ 10^{10}$**	10^{8}-10^{9}
Thickness to absorb 90% of 60keV incident radiation (cm)	130	2.6	2.6	**0.5**	0.5

✓ High atomic number

Good absorption efficiency

✓ Optimal band gap

Room Temperature Operation

✓ High $\mu\tau$ product

Spectroscopic detectors

Large area detectors

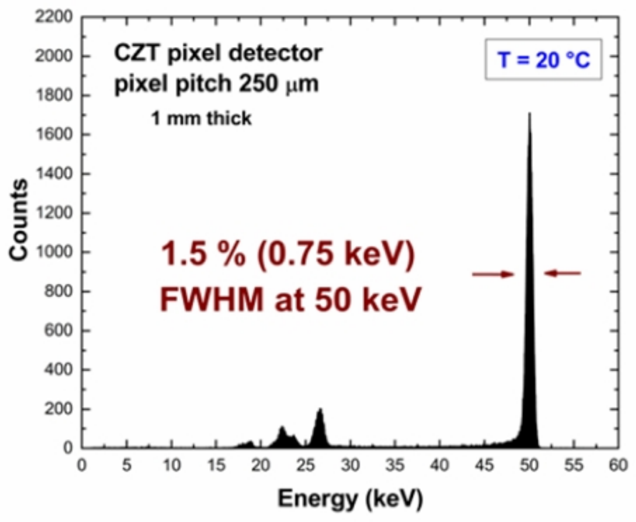

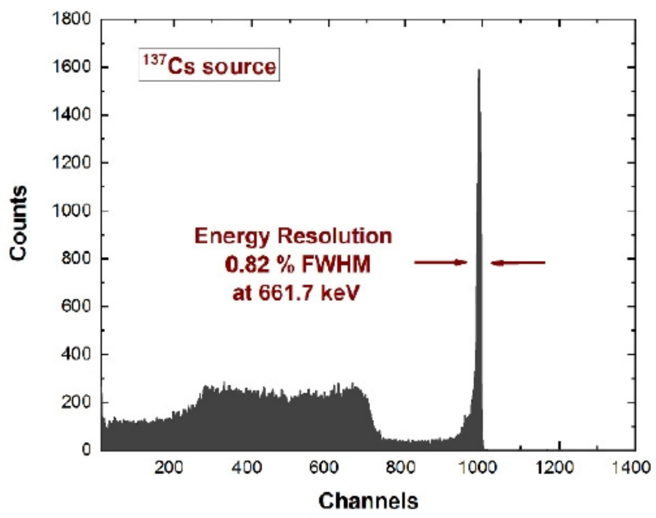

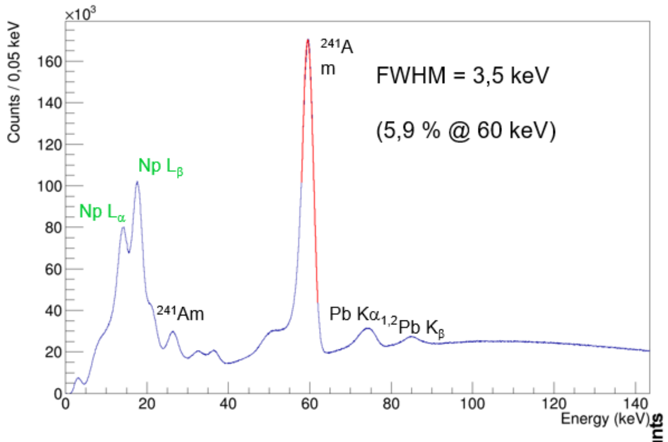

Good resolutions are confirmed

Small worsening only due to 30 m long cables in DAFNE (to be modified in the future)

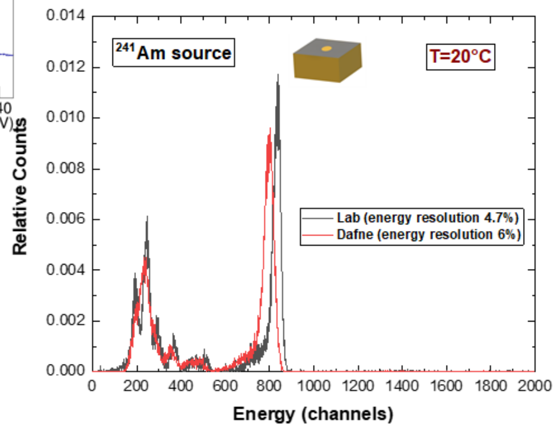

First tests in an accelerator environment

Linearity is preserved over a wide energy range

- Room temperature operation;
- Wide energy range: From few keV to MeV;
- High absorption efficiency
  - 1mm thick detectors >98% at 60keV
  - 10mm thick detectors >86% at 200keV
- High energy resolution:
  - 1.5 % at 50 keV
  - 0.82 % at 660 keV
- Fast detector response: down to 50 ns

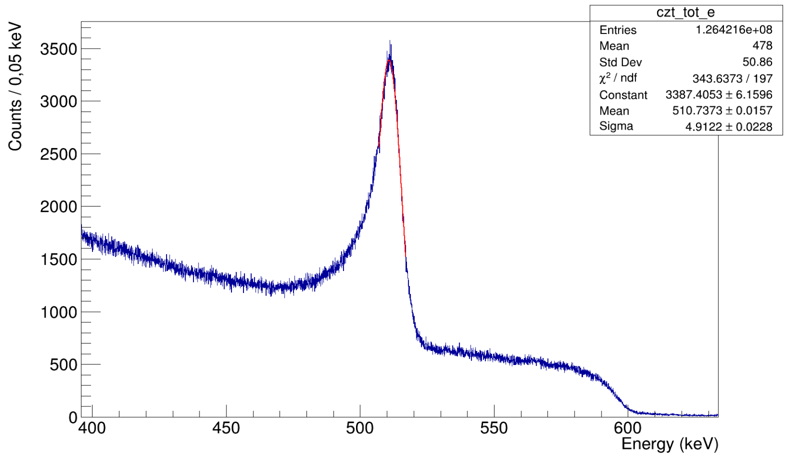

FWHM = 11,6 keV

(2,2 % @ 511 keV)

Nuclear Physics: Push the exotic atom spectroscopy to higher Z elements

Particle physics: Large area devices (> 1 cm^2) with a fine spatial resolution (< 100 μm) and optimal energetic resolution.

Astrophysics: measurement in the keV to MeV energy band (gamma and Compton telescope);

Medical imaging: SPECT (Single Photon Emission Computed Tomography) or CT (Computed Tomography);

Environmental monitoring: Radiological and Nuclear (RN) agents detection. Smart radiation detectors that detect, measure, identify and analyses gamma ray emitting radioactive sources;

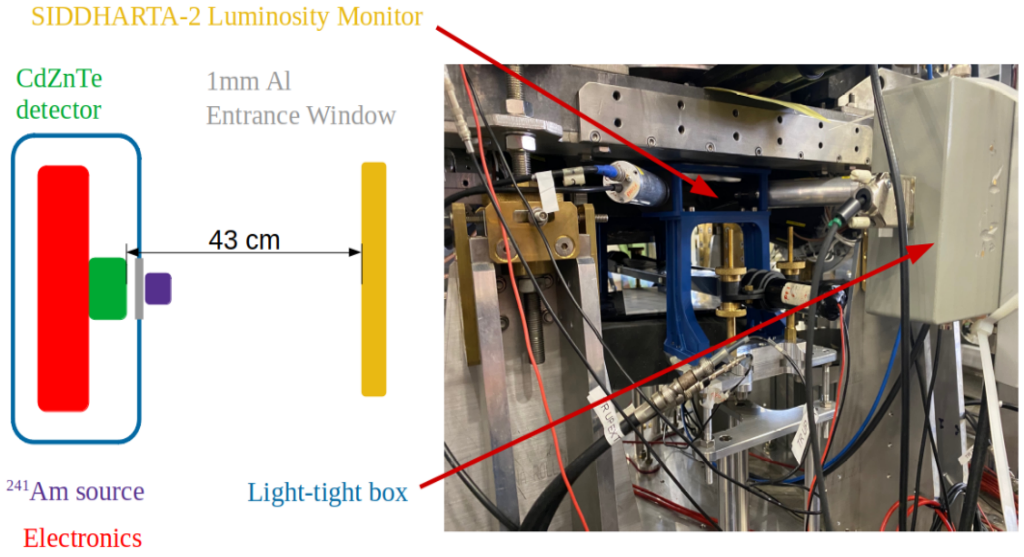

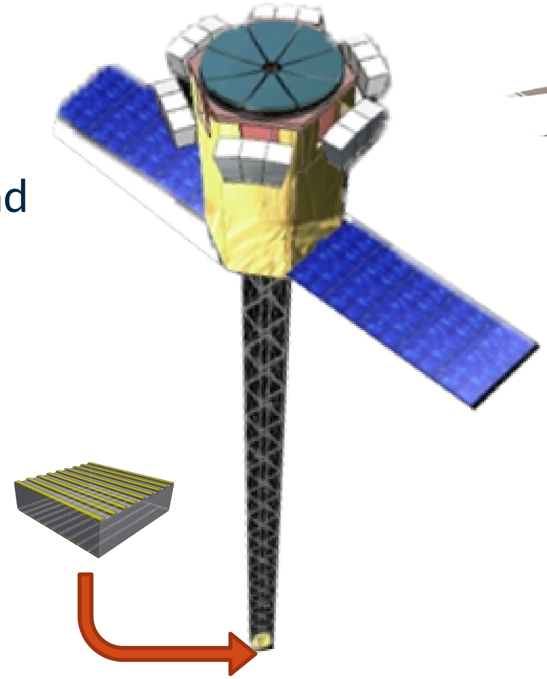

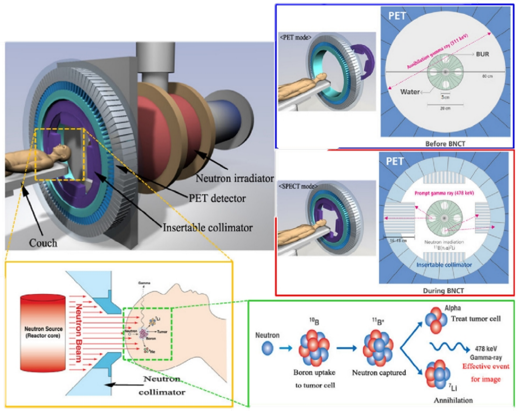

A. Bergamaschi, PSI
G. Tinti, LNF

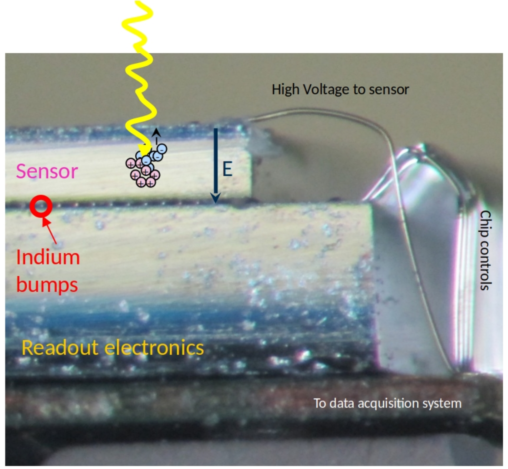

Wirebonding, Bumpbonding, deposition or wafer-to-wafer bonding for interconnection sensor to readout

The sensor material can be optimized for direct conversion for various energy ranges

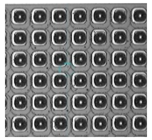

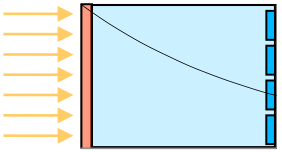

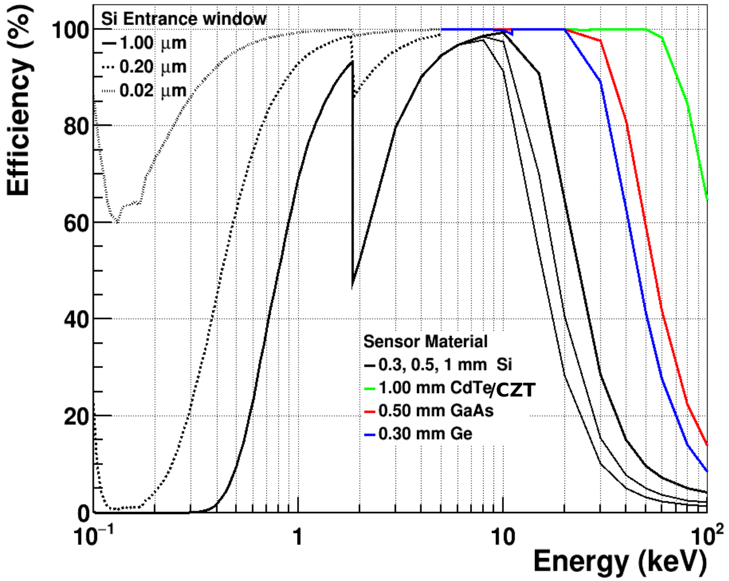

LGADs (Low Gain Avalanche Diodes) and sensor with thin entrance window
(0.2->2 keV)

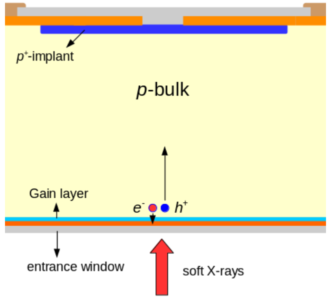

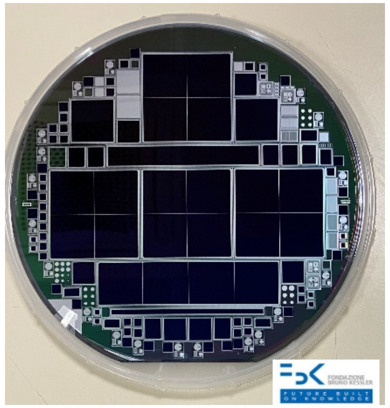

Planar silicon of various thicknesses
(3->20 keV)

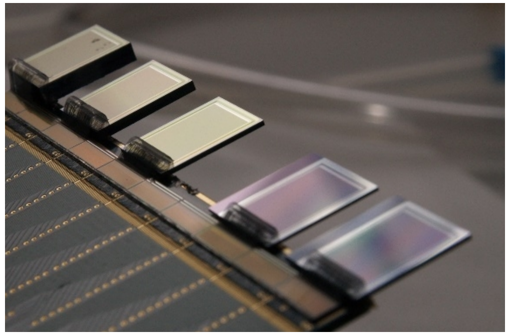

GaAs/ CZT/Perovskites
(20->150 keV)

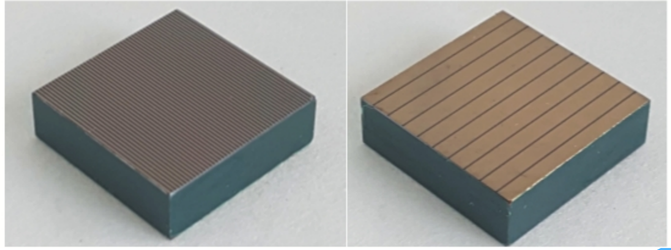

- Pixels and microstrip detectors depending on the application
  - Pixel pitch down to 25 microns (standard 75 microns)
  - Strip pitch 25-50 microns

- Single photon resolution, high dynamic range
  - Photon counting for synchrotrons
  - Charge integrating with dynamic gain switching for XFELs

- Different sensors for different energy ranges
  - Silicon 0.3-1 mm thick for 2-20 keV
  - LGADs with thin entrance window for 0.1-2 keV
  - High-Z materials (GaAs, CZT) for > 20keV

- Large area
  - Up to 16 Milion pixels

- Fast frame rate:
  - Fully parallel readout
  - Up to 25 kHz per module
  - Dedicated data backend required

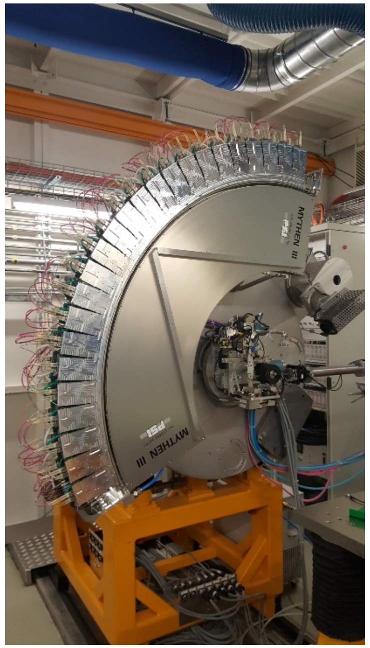

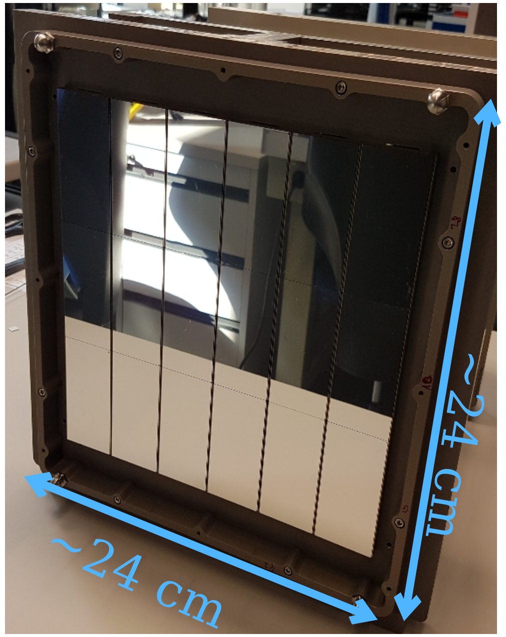

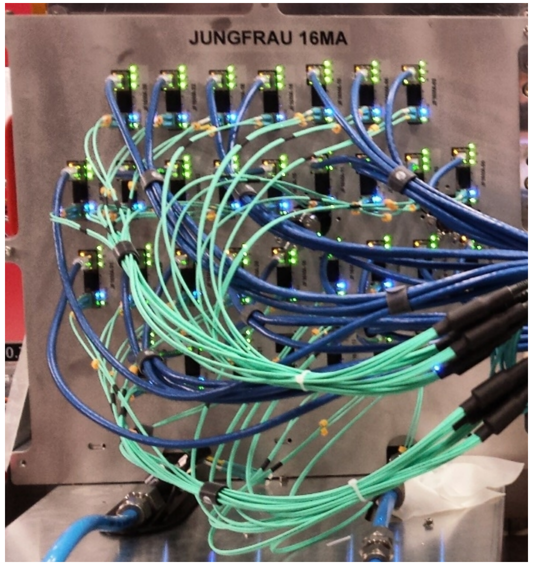

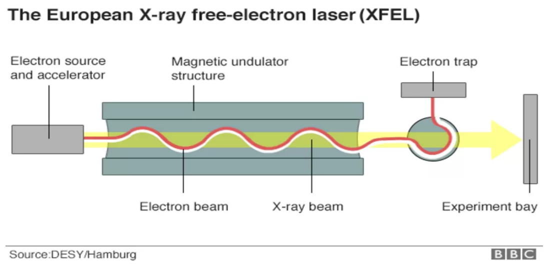

Diffraction and imaging (in situ) experiments

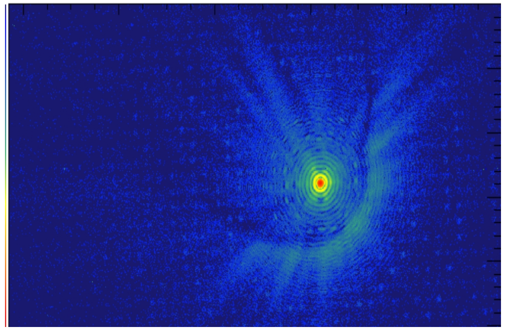
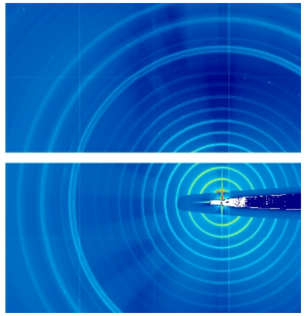
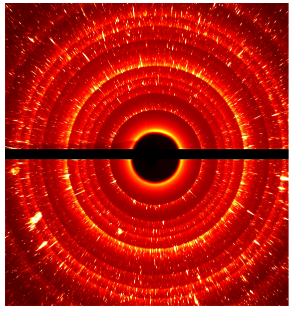

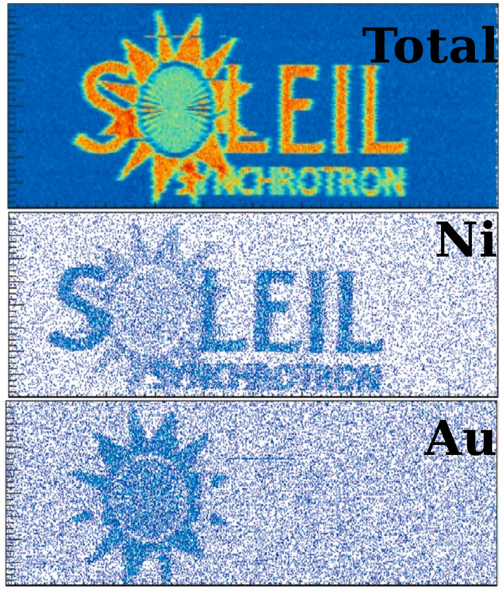

Energy resolved imaging (ca. 1 keV FWHM)

High resolution imaging using interpolation

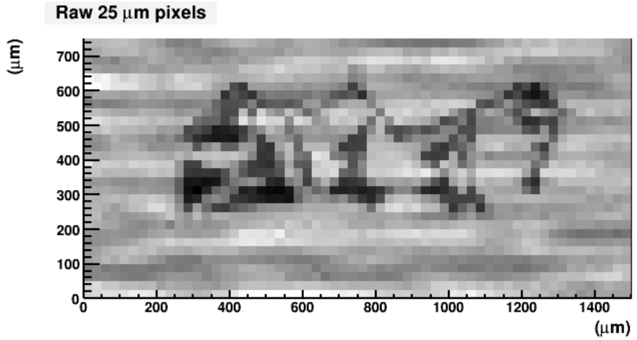

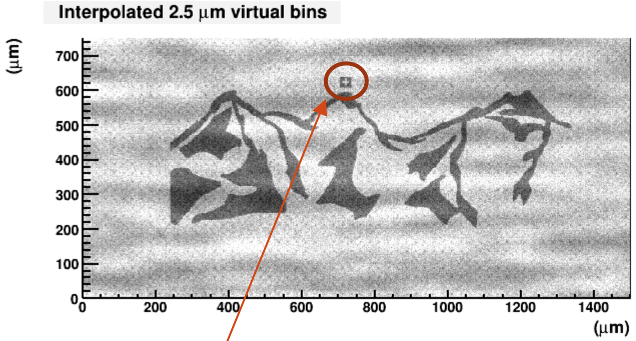

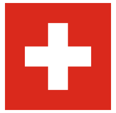

Main applications:

Diffraction (e.g, protein crystallography) and powder diffraction

Ptychography, microscopy technique with a few nm resolution enabled by hybrid detectors.

Combine position resolution with a moderate energy resolution ca. 1 keV FWHM

Exploiting the 25um pixels of Moench we can interpolate the position of single photons and achieve few microns resolution (size of the flag is 25um, the cross in the flag is 7um wide)

D. Mascali, LNS
E. Naselli, LNS

- *Optical Emission Spectroscopy;*
- *RF systems;*
- *InterferoPolarimetry;*
- *Gamma-ray detector array;*
- *Time- and Space-resolved X-ray spectroscopy*

for non-invasive
Magnetoplasma investigation

PANDORA (Plasma for Astrophysics, Nuclear Decay Observation and Radiation for Archaeometry) is a project supported by INFN, which aims to measure β-decays of nuclear astrophysical interest for the first time in laboratory plasmas emulating some stellar-like conditions.

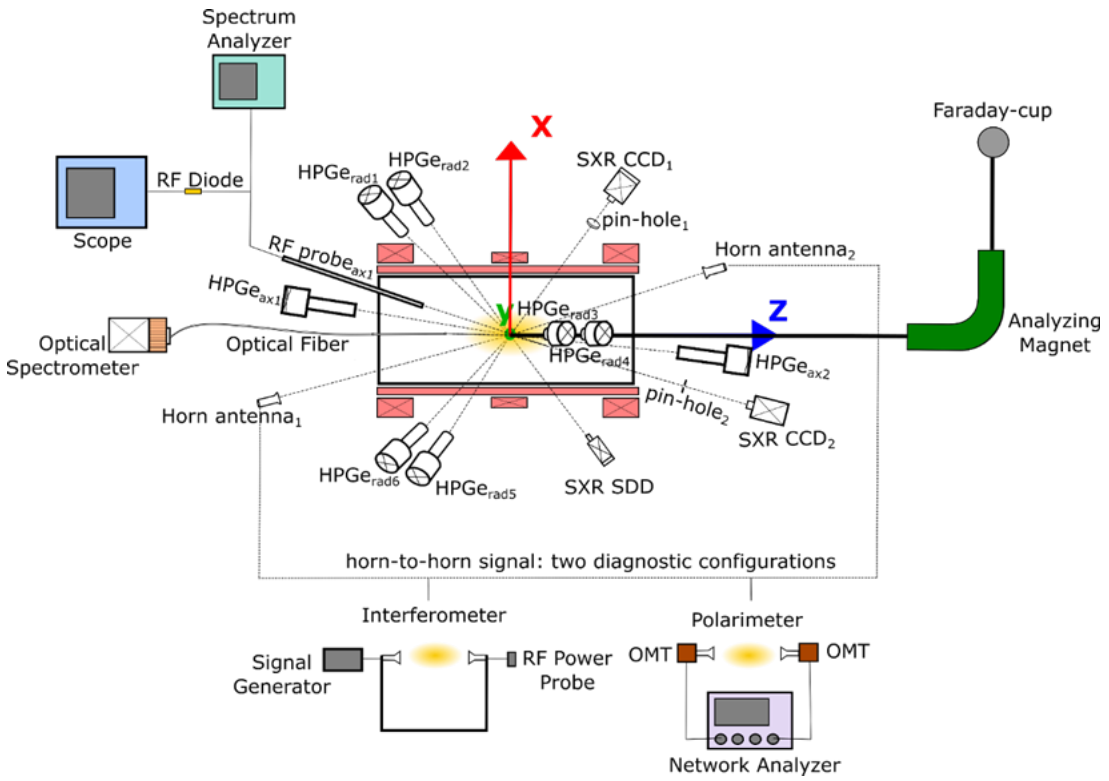

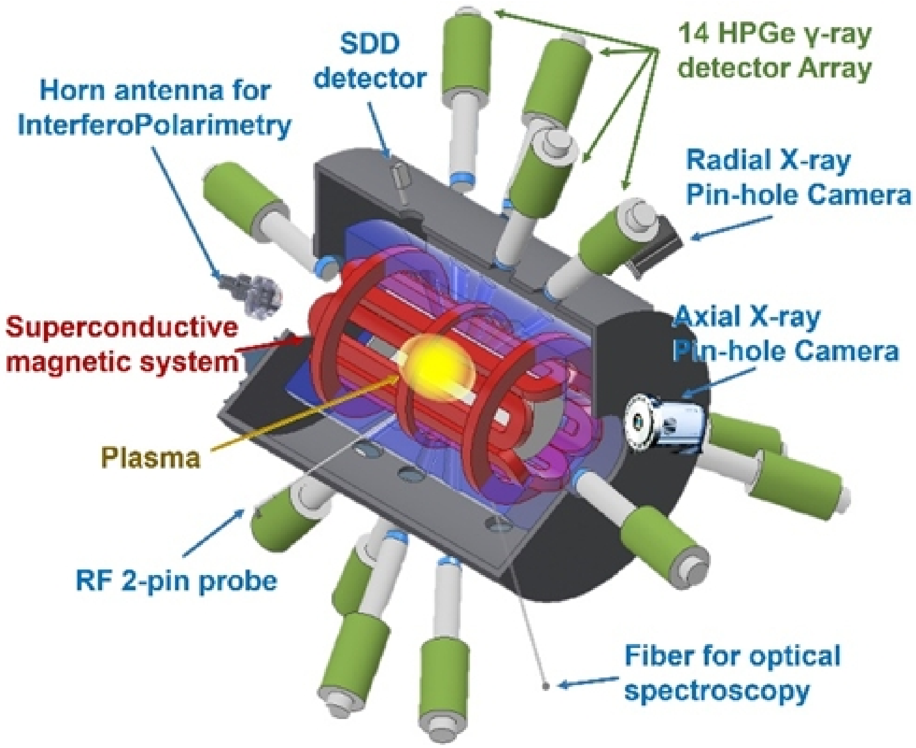

GOAL: correlate plasma parameters to nuclear activity of in-plasma β-decaying isotopes of nuclear astrophysics interest

D. Mascali et al., Universe 2022, 8(2)

Diagnostic tool	Sensitive Range	Measurement	Resolution - Measure Error
SDD	1 ÷ 30 keV	Volumetric soft X-ray Spectroscopy: warm electrons temperature and density	Resolution ~ 120 eV ε_{ne} ~ 7%, ε_{Te} ~ 5%
HPGe detector	30 ÷ 2000 keV	Volumetric hard X-ray Spectroscopy: hot electrons temperature and density	FWHM @ 1332.5 keV < 2.4 keV ε_{ne} ~ 7%, ε_{Te} ~ 5%
Visible Light Camera	1 ÷ 12 eV	Optical Emission Spectroscopy: cold electrons temperature and density	Δλ = 0.035 nm R = 13900
X-ray pin-hole camera	2 ÷ 15 keV	2D Space-resolved spectroscopy: soft X-ray Imaging and plasma structure	Energy Resolution ~ 0.3 keV Spatial Resolution ~ 0.5 mm
W-band super-heterodyne polarimeter	W-band 90 ÷ 100 GHz	Plasma-induced Faraday rotation: line-integrated electron density	ε_{ne} ~ 25%
Microwave Imaging Profilometry (MIP)	60 ÷ 100 GHz	Electron density profile	ε_{ne} ~ 1% ÷ 13%
Multi-pins RF probe	10 ÷ 26.5 GHz	Local EM field intensity	ε ~ 0.073 ÷ 0.138 dB
Multi-pins RF probe + Spectrum Analyzer (SA)	10 ÷ 26.5 GHz (*probe range*)	Frequency-domain RF wave	SA Resolution bandwidth: RBW = 3 MHz
Multi-pins RF probe + Scope + HPGe detector	10 ÷ 26.5 GHz (*probe range*)	Time-resolved radiofrequency burst and X-ray time-resolved Spectroscopy	80 Gs/s (*scope*) time scales below ns
Thomson Scattering	0.5 ÷ 500 eV	EEDF, absolute electron density global electron drift velocity	Condition-dependent (a function of spectral width, dependent on temperature, and area, dependent on density)

E. Naselli et al., Journal of Instrumentation 14 (2019) C10008

Several X-ray detectors will be used simultaneously:

- A SDD for volumetric spectroscopy in soft X-ray domain;
- Two CCD cameras with pin-hole systems, multi-disks collimators and shutters for imaging and space-resolved spectroscopy in the soft X-ray domain. A CCD camera will be radially installed, the other one axially;
- An array of 14 HPGe detectors for volumetric spectroscopy in hard X-ray domain and for γ-ray tagging;

Spatially-resolved X-ray Spectroscopy

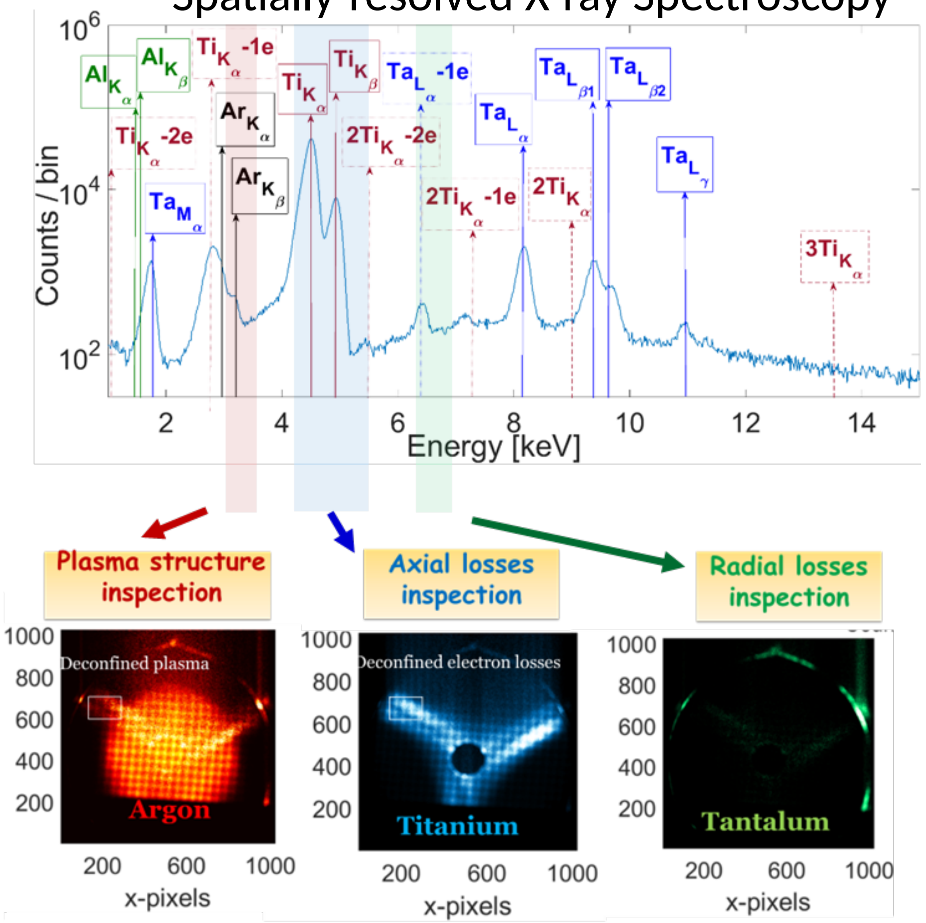

Energy resolution:
~ 230 eV @ 8 keV

Spatial resolution:
~ 400 µm

Spectrally-resolved X-ray Imaging

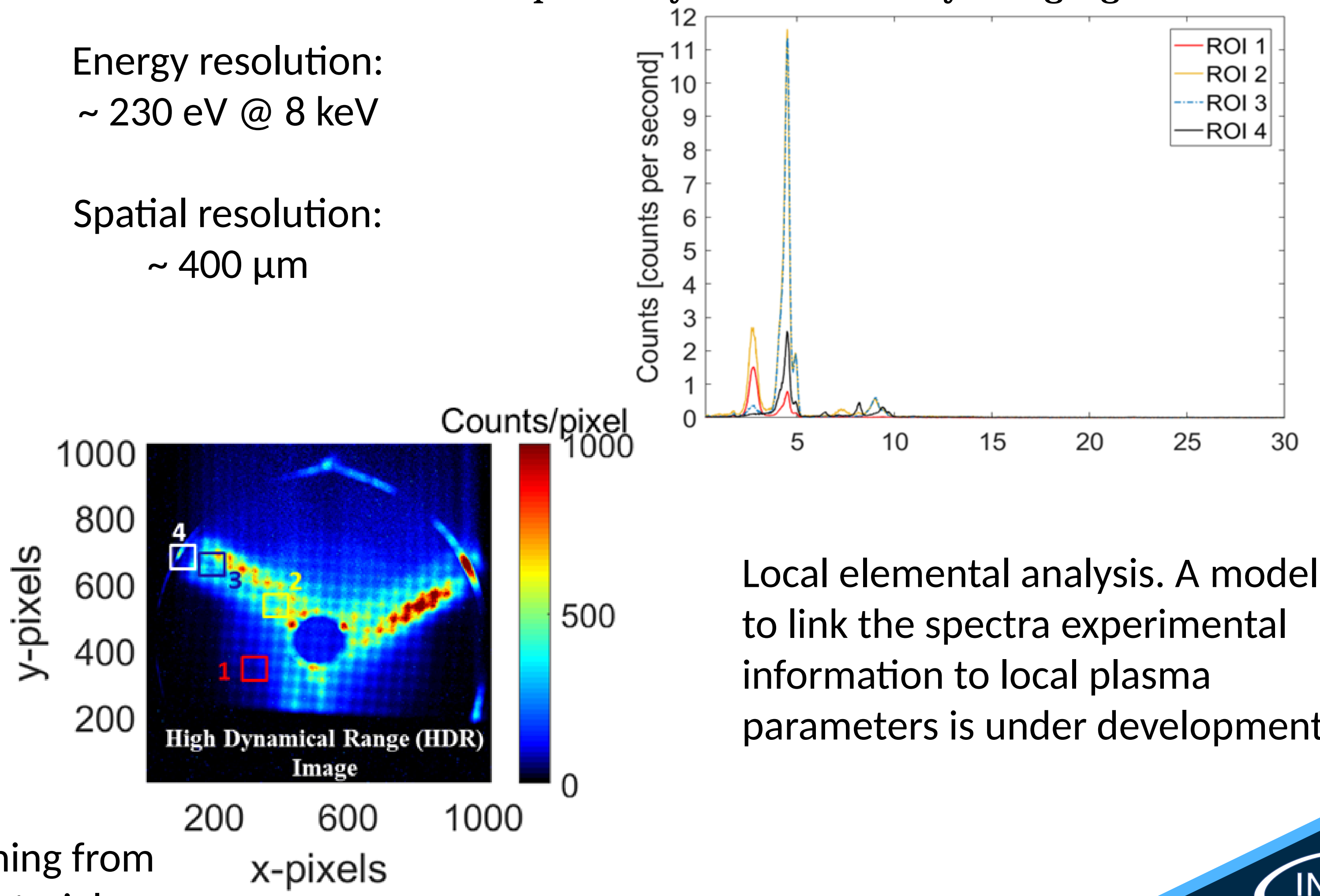

Local elemental analysis. A model to link the spectra experimental information to local plasma parameters is under development.

Single photon counted images showing X-rays coming from Ar plasma (red) and from plasma chamber wall material: Ti (blue) and Ta (green).
--> investigate the plasma spatial structure and the local balance between plasma vs. losses emissions.

E. Naselli et al., JINST (2022) **17** C01009
B. Mishra et al., Physics of Plasmas 28, 102509 (2021)

M. Testa, LNF

- **Organo Metal-Halide Perovskites** are a class of hybrid organic-inorganic semiconductor materials with a perovskite unit-cell structure **ABX$_3$** with
  - A = $CH_3NH_3^+$,B = metallic cation (Pb^{2+}), X= halide anions (Cl^-, Br^-,I^-)

- Opto-electronic properties combine **advantages from organic and inorganic semiconductors**

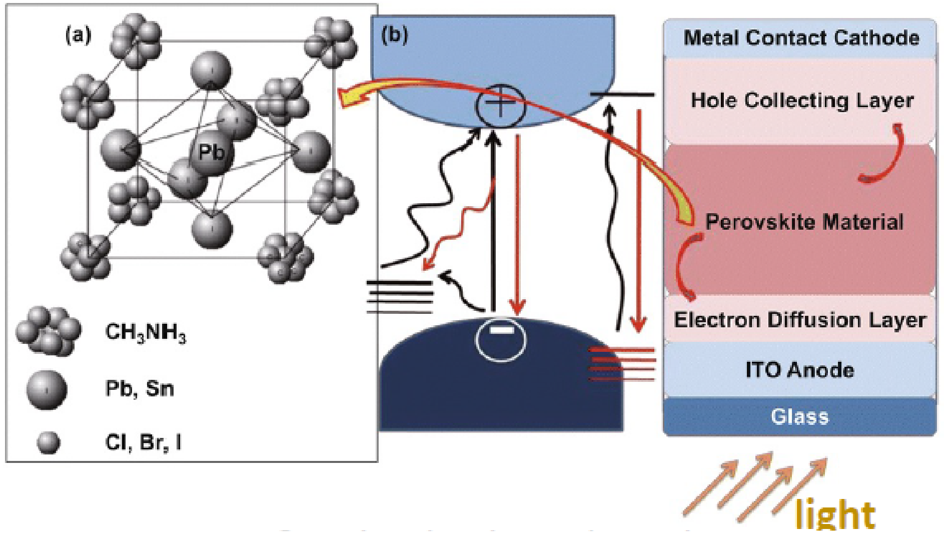

OMHPs combine the advantages of inorganic and organic semiconductors.

		Silicon	$CH_3NH_3Pb(I,Br)_3$
Density		2.33 g/cm^3	4.15 g/cm^3
Band gap (eV)		1.12 (indirect)	1.5-1.6 / 2.24 (direct)
Mobility (cm^2/Vs)	electrons	1400	< 70/190
	holes	450	< 160/220
Absorption (cm^{-1})		< 10^4	> 4x10^4
Threshold energy for impact ionization (eV)		1.2	~2 / 2.5 (estimated)
Mean free path (nm)		≤ 100	~100 (theory)

CH3PbBr3 crystal produced in PEROV INFN project

Technology and Thickness	Pro	Contra
Film 300 nm thickness 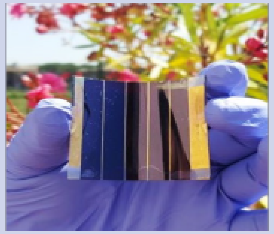	• large area • small transit time due to low thickness • flexible substrate	• polycristalline • grain boundaries • large variability between samples
Micro channels 2-6 microns realized 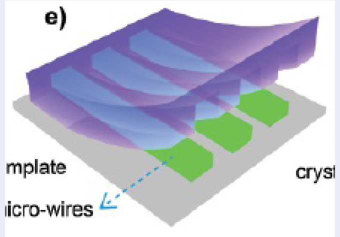	• large flexibility in dimension • moderate area • pixelization • flexible substrate • Deposited directly on substrate	• need high optimization of parameters (pressure, temperature)
Single crystals Up 0.5 cm realized 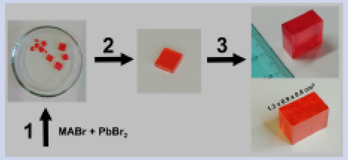	• ideal for single crystal large dimension, up to O(1) cm^3 • low defects	• No scalability to large area systems • Need to be cut mechanically for low thickness

Adaptable for direct X-ray detection

Micro-channels

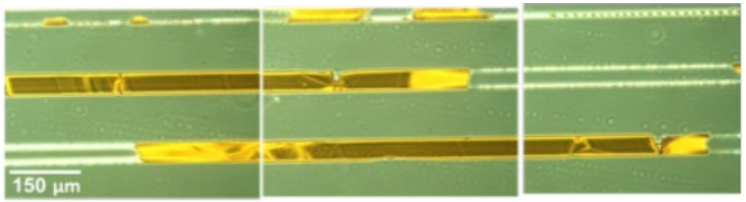

Typical dimension: W x L x H = 150 µm x 500 µm x 6(2) µm

Device realized with CH_3NH_3PbBr deposition on **patterned** Indium Tin Oxide/ $CH_3NH_3PbBr_3$ and Au evaporation

- Innovative technique
- *Deposited patent (INFN + CNR)* 102022000010469 (*)

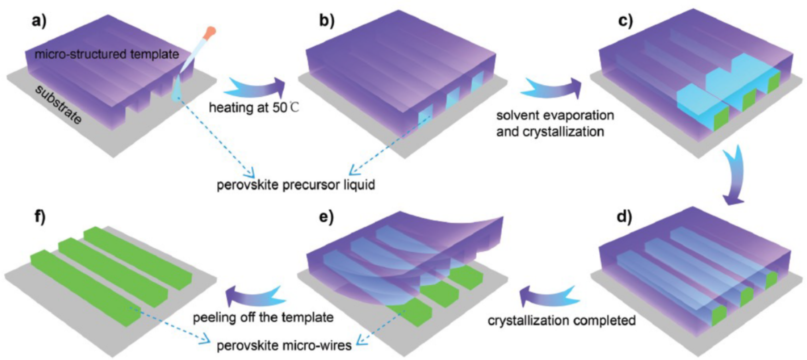

Pro:
- **large flexibility in dimension**
- **moderate area**
- **pixelization**
- **flexible substrate**
- **Deposited directly on substrate**

Contra:
- **need high optimization of parameters (pressure, temperature,..)**

(*) M. Testa, I. Viola, L.De Marco, M. Auf der Maur, F. Matteocci

Large bulk crystals

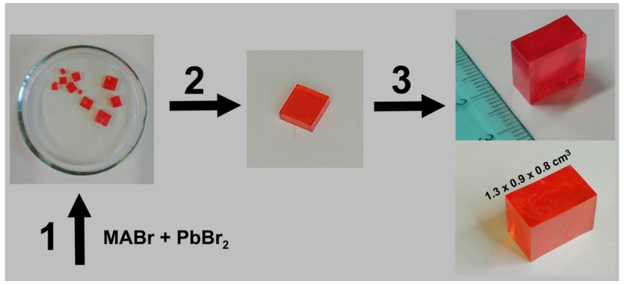

Contra:
- **No scalability to large area**
- **Need to be cut mechanically for low thickness**

Pro:
- **ideal for single crystal large dimension, up to O(1) cm^3**
- **low defects**

Dimensions up to 1.0 x 1.5 cm^2 and up to 0.5 cm thick down to 300 µm

Device realized with Indium Tin Oxide / $CH_3NH_3PbBr_3$ / Au

Due to large thickness, suited for radiation detection

Thanks